11

Antennas and Radiating Systems

11–1 Introduction

In Chapter 8 we studied the propagation characteristics of plane electromagnetic waves in source-free media without considering how the waves were generated. Of course, the waves must originate from sources, which in electromagnetic terms are time-varying charges and currents. In order to radiate electromagnetic energy efficiently in prescribed directions, the charges and currents must be distributed in specific ways. *Antennas* are structures designed for radiating electromagnetic energy effectively in a prescribed manner. Without an efficient antenna, electromagnetic energy would be localized, and wireless transmission of information over long distances would be impossible.

An antenna may be a single straight wire or a conducting loop excited by a voltage source, an aperture at the end of a waveguide, or a complex array of these properly arranged radiating elements. Reflectors and lenses may be used to accentuate certain radiation characteristics. Among radiation characteristics of importance are field pattern, directivity, impedance, and bandwidth. These parameters will be examined when particular antenna types are studied in this chapter.

To study electromagnetic radiation, we must call upon our knowledge of Maxwell's equations and relate electric and magnetic fields to time-varying charge and current distributions. A primary difficulty of this task is that the charge and current distributions on antenna structures resulting from given excitations are generally unknown and very difficult to determine. In fact, the geometrically simple case of a straight conducting wire (linear antenna) excited by a voltage source in the middle[†] has been a subject of extensive research for many years, and the exact charge and current distributions on a wire of a finite radius are extremely complicated even when the wire is assumed to be perfectly conducting. Fortunately, the radiation field

---

[†] This arrangement is called a *dipole antenna*.

of such an antenna is relatively insensitive to slight deviations in the current distribution, and a physically plausible approximate current on the wire yields useful results for nearly all practical purposes. We will examine the radiation properties of linear antennas with assumed currents.

By combining Maxwell's equations we can derive nonhomogeneous wave equations in **E** and in **H** (see Problem P.11-1). However, these equations tend to involve the charge and current densities in a complicated way. It is generally simpler to solve for the auxiliary potential functions **A** and V first. Using **A** and V in Eqs. (7-55) and (7-57), we can determine **H** and **E**. For harmonic time variation in a simple medium we have

$$\mathbf{H} = \frac{1}{\mu} \mathbf{\nabla} \times \mathbf{A} \tag{11-1}$$

and

$$\mathbf{E} = -\mathbf{\nabla}V - j\omega\mathbf{A}. \tag{11-2}$$

The potential functions **A** and V are themselves solutions of nonhomogeneous wave equations, Eqs. (7-63) and (7-65), and the solutions are given in Eqs. (7-78) and (7-77), respectively. For harmonic time dependence the **phasor retarded potentials** are, from Eqs. (7-100) and (7-99),

$R \triangleq |\vec{r} - \vec{r}'|$

$\begin{cases} A(\vec{r}) = \dfrac{\mu}{4\pi} \displaystyle\int_{V'} \dfrac{J(\vec{r}') e^{-jkR}}{R} dv' \\[4mm] V(\vec{r}) = \dfrac{1}{4\pi\varepsilon} \displaystyle\int_{V'} \dfrac{\rho(\vec{r}') e^{-jkR}}{R} dv' \end{cases}$

$$\mathbf{A} = \frac{\mu}{4\pi} \int_{V'} \frac{\mathbf{J}e^{-jkR}}{R}\, dv', \tag{11-3}$$

$$V = \frac{1}{4\pi\epsilon} \int_{V'} \frac{\rho e^{-jkR}}{R}\, dv', \tag{11-4}$$

$jk = \alpha + j\beta$

where $k = \omega\sqrt{\mu\epsilon} = 2\pi/\lambda$ is the wavenumber. Of course, **A** and V are related by the Lorentz condition, Eq. (7-98), for potentials, just as **J** and ρ are related by the equation of continuity Eq. (7-48), or

$$\mathbf{\nabla} \cdot \mathbf{J} = -j\omega\rho. \tag{11-5}$$

Hence there is no need for evaluating the integrals in both Eqs. (11-3) and (11-4). As a matter of fact, since **E** and **H** are related by Eq. (7-104b),

$$\mathbf{E} = \frac{1}{j\omega\epsilon} \mathbf{\nabla} \times \mathbf{H}. \tag{11-6}$$

We follow three steps in the determination of electromagnetic fields from a current distribution: (1) determine **A** from **J** using Eq. (11-3); (2) find **H** from **A** using Eq. (11-1); and (3) find **E** from **H** using Eq. (11-6). Note that only Step 1 requires an integration and that Steps 2 and 3 involve only straightforward differentiation. This is the procedure we will use in finding the radiation pattern of antennas.

We will first study the radiation fields and characteristic properties of an elemental electric dipole and of a small current loop (or magnetic dipole). We then consider finite-length thin linear antennas, of which the half-wavelength dipole is an important special case. The radiation characteristics of a linear antenna are largely determined by its length and the manner in which it is excited. To obtain more

directivity and other desirable properties, a number of such antennas may be arranged together to form an **antenna array**. The geometrical configuration, the spacings between the array elements, as well as the relative amplitudes and phases of the excitations in the elements all affect the field pattern of the array. Some basic properties of simple arrays will be considered.

When an antenna is used as a receiving device, its function is to collect energy from an incoming electromagnetic wave and deliver it to a receiver. Any antenna that is useful for radiation is also useful for reception. We will use the reciprocity theorem to show that the pattern, directivity, input impedance, effective height, and effective aperture of an antenna are the same for transmitting as for receiving. We will define backscatter cross section and study the radar equation and the effect of wave propagation near the earth's surface. Finally, we will discuss such antenna types as traveling-wave antennas, Yagi-Uda antennas, helical antennas, broadband antennas and arrays, and aperture antennas.

11–2 Radiation Fields of Elemental Dipoles

In this section we study the radiation fields of the simplest types of all radiating systems—namely, elemental oscillating electric and magnetic dipoles. We will find that the field solutions for electric and magnetic dipoles are duals of each other. As a consequence, the radiation properties of one can be deduced from those of the other without recalculation.

$d\ell \angle \angle \lambda$

wire of negligible $(\Rightarrow \vec{D} = 0)$ capacitance + uniform current

11–2.1 THE ELEMENTAL ELECTRIC DIPOLE

Consider the elemental oscillating electric dipole (in free space), as shown in Fig. 11–1, which consists of a short conducting wire of length $d\ell$ terminated in two small conductive spheres or disks (capacitive loading). We assume the current in the wire to be uniform and to vary sinusoidally with time:

$$i(t) = I \cos \omega t = \mathcal{R}e[Ie^{j\omega t}]. \tag{11–7}$$
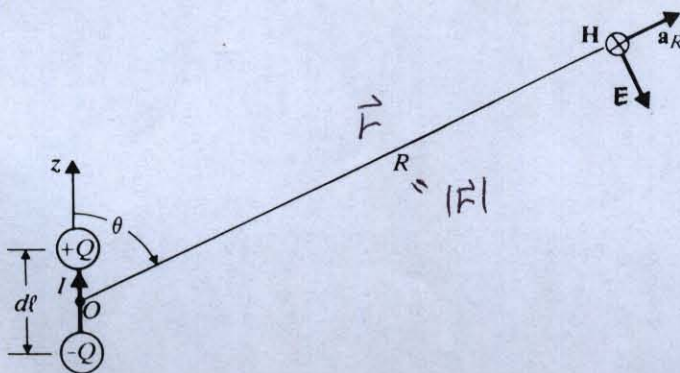
$$\vec{A}(\vec{r}) = \frac{\mu_0}{4\pi} \int_{-\frac{d\ell}{2}}^{\frac{d\ell}{2}} \frac{I(z') e^{j\beta R'}}{R'} dz'$$

where $R' \triangleq |\vec{r} - z'\vec{a}_z|$

$\beta \triangleq \frac{2\pi}{\lambda}$

FIGURE 11–1
A Hertzian dipole.

From (11-53), $\quad R' \simeq R - z' \cos\theta \simeq R \quad$ if $R \gg d\ell$

$I(z') \simeq I \qquad$ if $\lambda \gg d\ell$

$e^{j\beta R'} \simeq e^{j2\pi(R - z'\cos\theta)/\lambda} \simeq e^{j2\pi R/\lambda}$

$\simeq e^{j\beta R} \qquad$ if $R \gg d\ell$ or $\lambda \gg d\ell$

Since the current vanishes at the ends of the wire, charge must be deposited there. The relation between the charge and the current is

$$i(t) = \pm \frac{dq(t)}{dt}. \qquad \Rightarrow \text{ Equation of continuity satisfied}$$

$$\nabla \cdot J = -\frac{\partial f}{\partial t}$$

(11-8)

In phasor notation, $q(t) = \mathscr{R}e[Qe^{j\omega t}]$, we have

$$I = \pm j\omega Q \qquad (11-9)$$

or

$$Q = \pm \frac{I}{j\omega}, \qquad (11-10)$$

where, for the indicated current direction in Fig. 11-1, the positive sign is for the charge on the upper end and the negative sign for the charge on the lower end. The pair of equal and opposite charges separated by a short distance effectively form an electric dipole with a vector phasor electric moment

$$\mathbf{p} = \mathbf{a}_z Q \, d\ell \qquad (C \cdot m). \qquad (11-11)$$

Such an oscillating dipole is called a **Hertzian dipole**.

To determine the electromagnetic field of a Hertzian dipole, we follow the three steps outlined in Section 11-1. The phasor representation of the retarded vector potential is, from Eq. (11-3),

$$A(\vec{r}) = \frac{\mu_0}{4\pi} \int_{-d\ell/2}^{d\ell/2} \frac{I \, e^{-j\beta R}}{R} \, dz' \quad \Rightarrow \quad \mathbf{A} = \mathbf{a}_z \frac{\mu_0 I \, d\ell}{4\pi} \left(\frac{e^{-j\beta R}}{R} \right), \qquad (11-12)$$

where $\beta = k_0 = \omega/c = 2\pi/\lambda$. Since

$$\mathbf{a}_z = \mathbf{a}_R \cos\theta - \mathbf{a}_\theta \sin\theta, \qquad (11-13)$$

the spherical components of $\mathbf{A} = \mathbf{a}_R A_R + \mathbf{a}_\theta A_\theta + \mathbf{a}_\phi A_\phi$ are

$$A_R = A_z \cos\theta = \frac{\mu_0 I \, d\ell}{4\pi} \left(\frac{e^{-j\beta R}}{R} \right) \cos\theta, \qquad (11-14a)$$

$$A_\theta = -A_z \sin\theta = -\frac{\mu_0 I \, d\ell}{4\pi} \left(\frac{e^{-j\beta R}}{R} \right) \sin\theta, \qquad (11-14b)$$

$$A_\phi = 0. \qquad (11-14c)$$

From the geometry of Fig. 11-1 we expect no variation with respect to the coordinate ϕ. We have, from Eq. (2-139)

$$\mathbf{H} = \frac{1}{\mu_0} \nabla \times \mathbf{A} = \mathbf{a}_\phi \frac{1}{\mu_0 R} \left[\frac{\partial}{\partial R}(R A_\theta) - \frac{\partial A_R}{\partial \theta} \right]$$

$$= -\mathbf{a}_\phi \frac{I \, d\ell}{4\pi} \beta^2 \sin\theta \left[\frac{1}{j\beta R} + \frac{1}{(j\beta R)^2} \right] e^{-j\beta R}. \qquad (11-15)$$

The electric field intensity can be obtained from Eq. (11–6):

$$\mathbf{E} = \frac{1}{j\omega\epsilon_0} \nabla \times \mathbf{H}$$

$$= \frac{1}{j\omega\epsilon_0} \left[\mathbf{a}_R \frac{1}{R\sin\theta} \frac{\partial}{\partial\theta}(H_\phi \sin\theta) - \mathbf{a}_\theta \frac{1}{R}\frac{\partial}{\partial R}(RH_\phi) \right], \qquad (11-16)$$

which gives

$$E_R = -\frac{I\,d\ell}{4\pi}\eta_0\beta^2 2\cos\theta \left[\frac{1}{(j\beta R)^2} + \frac{1}{(j\beta R)^3} \right]e^{-j\beta R}, \qquad (11-16a)$$

$$E_\theta = -\frac{I\,d\ell}{4\pi}\eta_0\beta^2 \sin\theta \left[\frac{1}{j\beta R} + \frac{1}{(j\beta R)^2} + \frac{1}{(j\beta R)^3} \right]e^{-j\beta R}, \qquad (11-16b)$$

$$E_\phi = 0, \qquad (11-16c)$$

where $\eta_0 = \sqrt{\mu_0/\epsilon_0} \cong 120\pi\ (\Omega)$.

Equations (11–15) and (11–16) constitute the electromagnetic field of a Hertzian dipole. Note that in deriving these expressions we used only the current in the dipole to find the vector potential $\mathbf{A}$; the charges at the ends of the dipole did not enter into the calculations. We could, however, take an alternative approach by finding both $\mathbf{A}$ from $I\,d\ell$, as in Eq. (11–12), and the scalar potential V from the pair of equal and opposite charges using Eq. (11–4). The electric field intensity could then be determined from Eq. (11–2), instead of from Eq. (11–6). The result would be exactly the same as that obtained above (see Problem P.11–2).

The complete field expressions in Eqs. (10–15) and (10–16) are fairly complicated. It is advantageous to examine their behavior in regions near to and far from the dipole separately.

Near Field   In the region near to the Hertzian dipole (in the *near zone*), $\beta R = 2\pi R/\lambda \ll 1$, the leading term in Eq. (11–15) is

$$H_\phi = \frac{I\,d\ell}{4\pi R^2}\sin\theta, \qquad (11-17)$$

where we have approximated the factor $e^{-j\beta R} = 1 - j\beta R - (\beta R)^2/2 + \cdots$ by unity. Equation (11–17) is exactly what would be obtained for the magnetic field intensity due to a current element $I\,d\ell$ by applying the Biot-Savart law in magnetostatics as given in Eq. (6–33b).

The leading near-zone terms for the electric field intensity are, from Eqs. (11–16a) and (11–16b),

$$E_R = \frac{p}{4\pi\epsilon_0 R^3}2\cos\theta \qquad (11-18a)$$

and

$$E_\theta = \frac{p}{4\pi\epsilon_0 R^3}\sin\theta, \qquad (11-18b)$$

Handwritten annotations:

} Why? (next to paragraph about Hertzian dipole derivation)

} (Why?) (next to Biot-Savart law paragraph)

$$H = -\vec{a}_\phi \frac{I\,d\ell}{4\pi}\beta^2 \sin\theta \left[\underbrace{\left(\frac{1}{j\beta R}\right)}_{\ll} + \underbrace{\left(\frac{1}{(j\beta R)^2}\right)}_{\ll} \right] \times \underbrace{\left(e^{-j\beta R}\right)}_{\approx 1} \;(11\text{-}15) \;\Rightarrow H_\phi = \frac{I\,d\ell}{4\pi R^2}\sin\theta$$

(Why?)

quasi-static approximation

$$A(\vec{r}) = \frac{\mu}{4\pi}\int_{V'} \frac{J(\vec{r}')e^{-jkR}}{R}\,dv' \;\approx\; \frac{\mu}{4\pi}\int_{V'} \frac{J(\vec{r}')}{R}\,dv'$$

$$\Rightarrow H = \frac{1}{\mu}\nabla \times A(\vec{r}) = \text{Biot-Savart Law (by Helmholtz Theorem)}$$
in (6-33)

where the phasor relations (11–10) and (11–11) have been used. These expressions are identical to those of the electric field intensity due to an elemental electric dipole of a moment p in the z-direction, as given in Eq. (3–31), obtained by an application of the laws of electrostatics. The **near-zone fields** of an oscillating time-varying dipole are then **quasi-static fields**.

Far Field   The region where $\beta R = 2\pi R/\lambda \gg 1$ is the **far zone**. The far-zone leading terms in Eqs. (11–15) and (11–16) are

$$H = -\vec{a}_\phi \frac{I\,d\lambda}{4\pi} \beta^2 \sin\theta \times$$

$$\left[\frac{1}{j\beta R} + \frac{1}{(\beta R)^2}\right] e^{-j\beta R}$$

$$(11-15)$$

$\Rightarrow$

$$\boxed{H_\phi = j\frac{I\,d\ell}{4\pi}\left(\frac{e^{-j\beta R}}{R}\right)\beta \sin\theta \qquad \text{(A/m)},} \qquad (11\text{–}19\text{a})$$

$E_R = 0 \Rightarrow$
in (11–16a)

$$\boxed{E_\theta = j\frac{I\,d\ell}{4\pi}\left(\frac{e^{-j\beta R}}{R}\right)\eta_0 \beta \sin\theta \qquad \text{(V/m)}.} \qquad (11\text{–}19\text{b})$$

Several important observations can be made on these **far-zone fields**. First, E_θ and H_ϕ are in space quadrature and in time phase. Second, their ratio $E_\theta/H_\phi = \eta_0$ is a constant equal to the intrinsic impedance of the medium (which is, in the present case, free space). The far-zone fields, then, have the same properties as those of a plane wave. This is not unexpected, since at very large distances from the dipole a spherical wavefront closely resembles a plane wavefront.

A third observation from Eqs. (11–19a, b) is that the magnitude of the far-zone fields varies inversely with the distance from the source. The phase of both E_θ and H_ϕ is a periodic function of R with a period that is the wavelength:

$$\lambda = \frac{2\pi}{\beta} = \frac{c}{f}. \qquad (11\text{–}20)$$

Note that the far-zone condition $\beta R \gg 1$ translates into $R \gg \lambda/2\pi$; hence one has to be farther away from the dipole at lower frequencies in order to be in the far zone. (Other characteristics of far-zone fields will be discussed in Section 11–3.)

11–2.2   THE ELEMENTAL MAGNETIC DIPOLE

Let us now consider a small filamentary loop of radius b carrying a uniform time-harmonic current $i(t) = I \cos \omega t$ around its circumference, as shown in Fig. 11–2. This is an elemental magnetic dipole with a vector phasor magnetic moment

$$i(t) = \text{Re}\left[I\,e^{j\omega t}\right] \qquad \mathbf{m} = \mathbf{a}_z I\pi b^2 = \mathbf{a}_z m \qquad (\text{A·m}^2). \qquad (11\text{–}21)$$

To determine the electromagnetic field, we first find the vector potential. The procedure is the same as that used in Section 6–5, except for the time-dependent nature of the current. Instead of starting from Eq. (6–39), we have

$$A(\vec{r}) = \frac{\mu}{4\pi}\int_{V'} \frac{J(\vec{r}')e^{-jkR}}{R}\,dv' \Rightarrow \qquad \mathbf{A} = \frac{\mu_0 I}{4\pi}\oint \frac{e^{-j\beta R_1}}{R_1}\,d\ell'. \qquad (11\text{–}22)$$
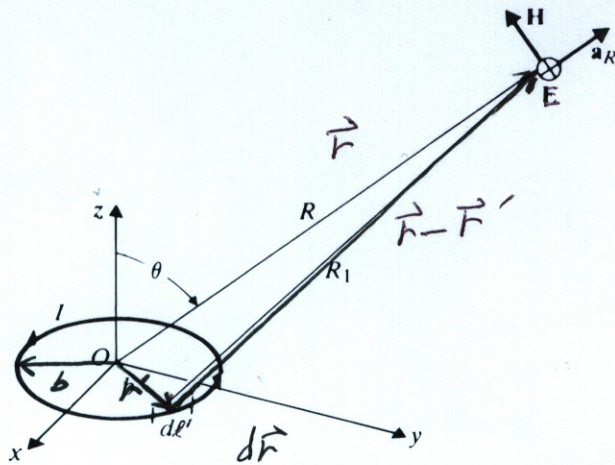
where
$$jk = \alpha + j\beta$$
$$J(\vec{r}')\,dv' = I\,d\ell'$$
$$R \triangleq |\vec{r} - \vec{r}'|$$

where
$$R_1 \triangleq |\vec{r} - \vec{r}'|$$

FIGURE 11-2
A magnetic dipole.

Here, $R = |\vec{r}|$

$R_1 = |\vec{r} - \vec{r}'|$

The integral in Eq. (11–22) is relatively difficult to carry out exactly because R_1 changes with the location of $d\ell'$ on the loop. For a small loop the exponential factor in the numerator can be written as

$$e^{-j\beta R_1} = e^{-j\beta R}e^{-j\beta(R_1 - R)}$$

$$\cong e^{-j\beta R}[1 - j\beta(R_1 - R)]. \qquad \text{if } b \ll \lambda \qquad (11\text{--}23)$$

$$(\because b \ll R)$$

Substitution of Eq. (11–23) in Eq. (11–22) yields approximately

$$A = \frac{\mu_0 I}{4\pi}\oint \frac{e^{-j\beta R_1}}{R_1}d\vec{\ell} \Rightarrow \quad A = \frac{\mu_0 I}{4\pi}e^{-j\beta R}\left[(1 + j\beta R)\oint \frac{d\ell'}{R_1} - j\beta\oint d\ell'\right]. \qquad \oint d\vec{r} = 0 \qquad (11\text{--}24)$$

$$(11\text{--}22)$$

The second integral in Eq. (11–24) obviously vanishes. The first integral is the same as that in Eq. (6–39), except for the multiplying factor $(1 + j\beta R)e^{-j\beta R}$. In view of the result in Eq. (6–43) we have $pp.\ 239\text{--}240$

$$A = \mathbf{a}_\phi \frac{\mu_0 m}{4\pi R^2}(1 + j\beta R)e^{-j\beta R}\sin\theta \qquad (11\text{--}25)$$

The electric and magnetic field intensities can be determined by straightforward differentiation using Eqs. (11–6) and (11–1), respectively:

$$E_\phi = \frac{j\omega\mu_0 m}{4\pi}\beta^2 \sin\theta\left[\frac{1}{j\beta R} + \frac{1}{(j\beta R)^2}\right]e^{-j\beta R}, \qquad (11\text{--}26a)$$

$$H_R = -\frac{j\omega\mu_0 m}{4\pi\eta_0}\beta^2 2\cos\theta\left[\frac{1}{(j\beta R)^2} + \frac{1}{(j\beta R)^3}\right]e^{-j\beta R}, \qquad (11\text{--}26b)$$

$$H_\theta = -\frac{j\omega\mu_0 m}{4\pi\eta_0}\beta^2 \sin\theta\left[\frac{1}{j\beta R} + \frac{1}{(j\beta R)^2} + \frac{1}{(j\beta R)^3}\right]e^{-j\beta R}. \qquad (11\text{--}26c)$$

Comparison of Eqs. (11–26a, b, c) with Eqs. (11–15) and (11–16a, b) reveals immediately the dual nature of the electromagnetic fields of electric and magnetic dipoles.

Let (E_e, H_e) denote the electric and magnetic fields of the electric dipole and (E_m, H_m) the electric and magnetic fields of the magnetic dipole. We have

$$E_e = \eta_0 H_m \tag{11-27}$$

and

$$H_e = -\frac{E_m}{\eta_0} \tag{11-28}$$

if the electric and magnetic dipole moments are related as follows:

$$I\,d\ell = j\beta m, \qquad \text{(Here, } d\ell \ll \lambda \Leftrightarrow b \ll \lambda) \tag{11-29}$$

where $\beta = \omega\mu_0/\eta_0 = \omega\sqrt{\mu_0\epsilon_0}$. Equations (11–27) and (11–28) are results expected from the principle of duality, which was introduced in connection with Example 7–7. Thus Hertzian electric dipole and elemental magnetic dipole are dual devices, and their electromagnetic fields are dual solutions of source-free Maxwell's equations. As a consequence of this duality, the discussions about the nature of the near and far fields of an electric dipole apply to the dual quantities of a magnetic dipole. In particular, the far-zone ($\beta R \gg 1$) fields of a magnetic dipole are

H_ϕ in
(11-19a)

$\dfrac{(11-28)}{(11-29)} \Longrightarrow$

$$\boxed{E_\phi = \frac{\omega\mu_0 m}{4\pi}\left(\frac{e^{-j\beta R}}{R}\right)\beta \sin\theta \quad \text{(V/m)},} \tag{11-30a}$$

E_θ in
(11-19b)

$\dfrac{(11-29)}{(11-29)} \Longrightarrow$

$$\boxed{H_\theta = -\frac{\omega\mu_0 m}{4\pi\eta_0}\left(\frac{e^{-j\beta R}}{R}\right)\beta \sin\theta \quad \text{(A/m)}.} \tag{11-30b}$$

We can see that the far-field intensities vary inversely as R and their ratio E_ϕ/H_θ equals the intrinsic impedance η_0 of free space.

Examination of the far-field E_θ in Eq. (11–19b) of the electric dipole and E_ϕ in Eq. (11–30a) of the magnetic dipole reveals that they have the same pattern function $|\sin\theta|$ and are in both space and time quadrature. Thus it is possible to combine electric and magnetic dipoles to form an antenna that produces circular polarization (see Problem P.11–4).

$$E_\theta = j\frac{I\,d\ell}{4\pi}\left(\frac{e^{-j\beta R}}{R}\right)\eta_0 \beta \sin\theta \tag{11-19b}$$

11–3 Antenna Patterns and Antenna Parameters

In antenna problems we are primarily interested in the far-zone fields. These are also called *radiation fields*. No physical antennas radiate uniformly in all directions in space. The graph that describes the relative far-zone field strength versus direction at a fixed distance from an antenna is called the *radiation pattern* of the antenna, or *antenna pattern*
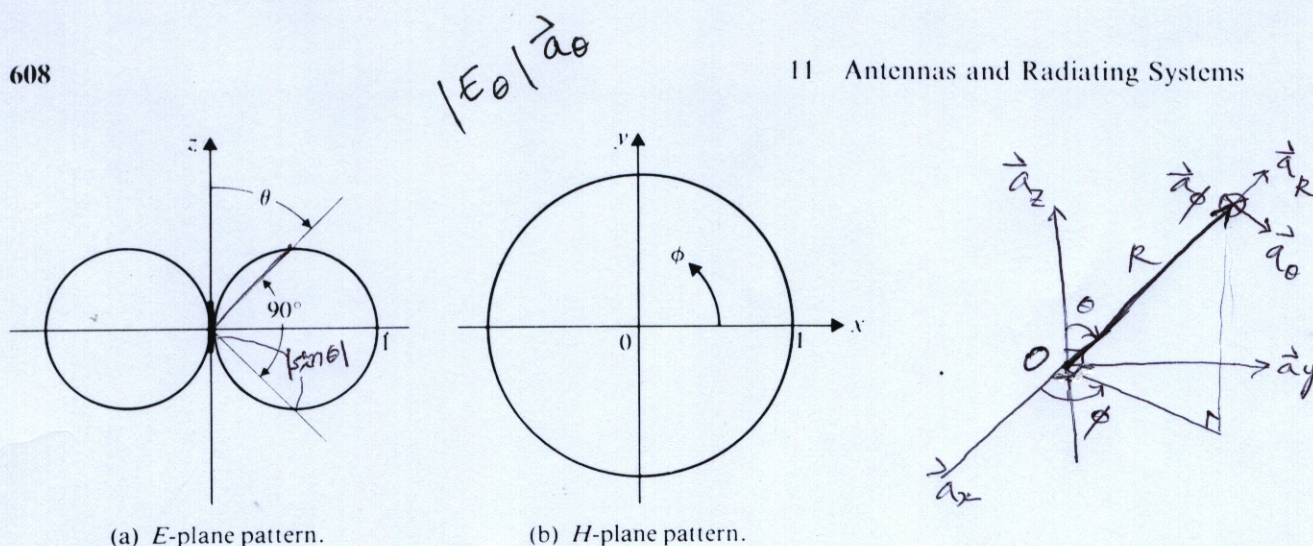
$|E_\theta|\vec{a}_\theta$

(a) *E*-plane pattern.   (b) *H*-plane pattern.

FIGURE 11–3
Radiation patterns of a Hertzian dipole.

---

simply the **antenna pattern**. In general, an antenna pattern is three-dimensional, varying with both θ and ϕ in a spherical coordinate system. The difficulties of making three-dimensional plots can be avoided—as is the usual practice—by plotting separately the magnitude of the normalized field strength (with respect to the peak value) versus θ for a constant ϕ (an **E-plane pattern**) and the magnitude of the normalized field strength versus ϕ for $\theta = \pi/2$ (the **H-plane pattern**).

EXAMPLE 11–1   Plot the *E*-plane and *H*-plane radiation patterns of a Hertzian dipole.

Solution   Since E_θ and H_ϕ in the far zone are proportional to each other, we need only consider the normalized magnitude of E_θ.

a) *E-plane pattern*. At a given R, E_θ is independent of ϕ; and from Eq. (11–19b) the normalized magnitude of E_θ is

$$\text{Normalized } |E_\theta| = |\sin\theta|. \qquad (11-31)$$

This is the *E*-plane **pattern function** of a Hertzian dipole. For any given ϕ, Eq. (11–31) represents a pair of circles, as shown in Fig. 11–3(a).

b) *H-plane pattern*. At a given R and for $\theta = \pi/2$ the normalized magnitude of E_θ is $|\sin\theta| = 1$. The *H*-plane pattern is then simply a circle of unity radius centered at the z-directed dipole, as shown in Fig. 11–3(b). ∎
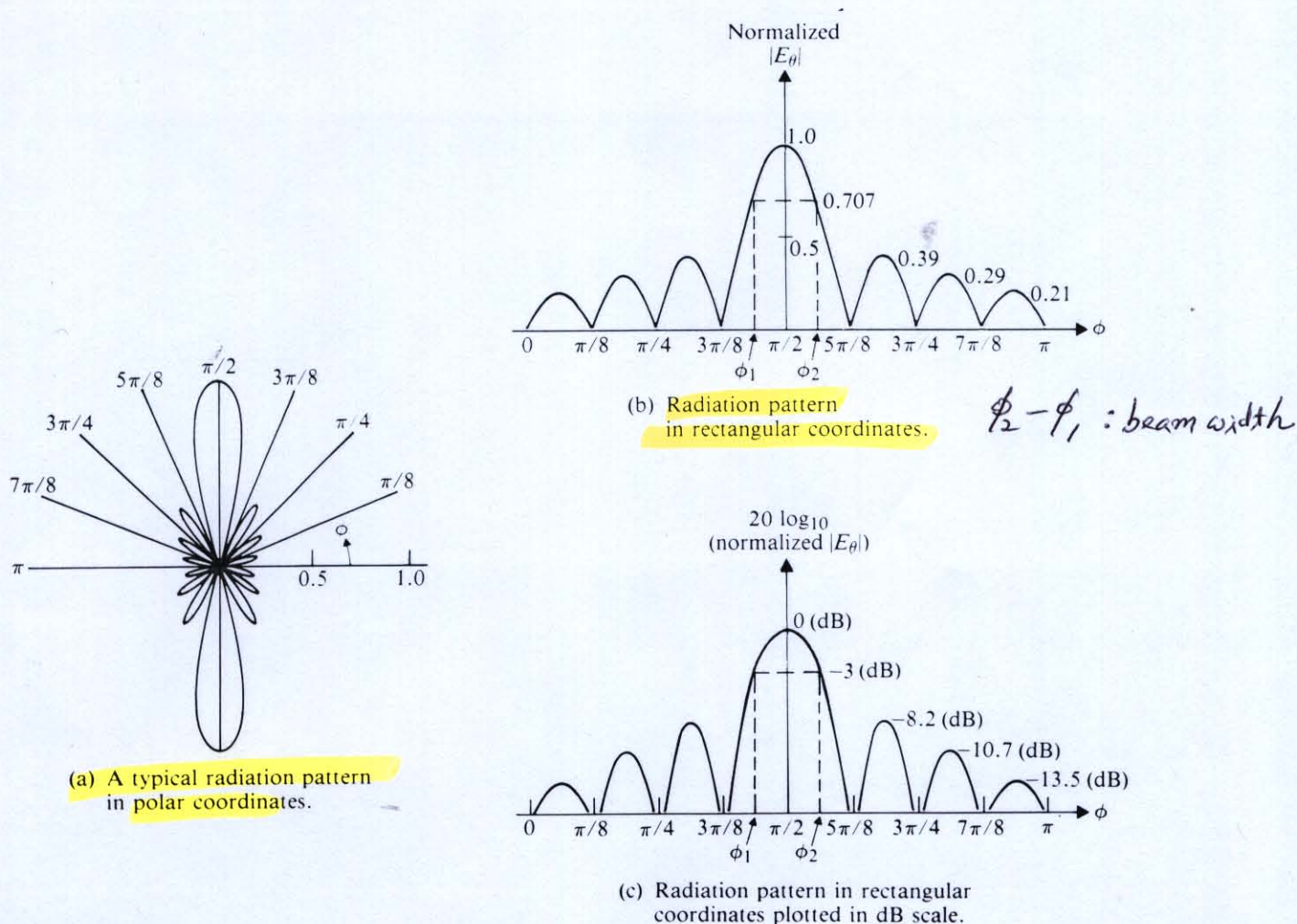
The radiation pattern of practical antennas are usually more complicated than those shown in Fig. 11–3. A typical *H*-plane pattern might look like the one illustrated in Fig. 11–4(a), which is plotted in polar coordinates with normalized $|E_\theta|$ versus ϕ. It generally has a major maximum and several minor maxima. The region of maximum

radiation between the first null points around it is the *main beam*, and the regions of minor maxima are *sidelobes*.

Sometimes it is convenient to plot antenna patterns in rectangular coordinates. The polar plot in Fig. 11-4(a) will appear as Fig. 11-4(b) in rectangular coordinates. Since the field intensities in the main-beam and sidelobe directions may differ by many orders of magnitude, antenna patterns are frequently plotted in a logarithmic scale measured in decibels down from the main-beam level. The pattern in Fig. 11-4(b) converted to a decibel scale will have the shape shown in Fig. 11-4(c).

In the comparison of various antenna patterns the following characteristic parameters are of importance: (1) width of main beam, (2) sidelobe levels, and (3) directivity.

(b) Radiation pattern in rectangular coordinates.

$\phi_2 - \phi_1$: beam width

(a) A typical radiation pattern in polar coordinates.

(c) Radiation pattern in rectangular coordinates plotted in dB scale.

FIGURE 11-4
Typical *H*-plane radiation patterns.

Solid Angles

l is the length of the arc subtending the angle. This definition is useful because l/r is independent of the radius of the circle. A similar procedure is used to define a solid angle. A typical solid angle is indicated by the irregular cone shown in Fig. 3–1. When two spheres of radii r_1 and r_2 are drawn with centers at the apex of this cone, areas s_1 and s_2 are inscribed by the cone on the surfaces of the respective spheres. Since these surfaces are proportional to the squares of the respective radii, the dimensionless ratio $s_1/r_1^2 = s_2/r_2^2 = \omega$ is independent of the size of the sphere and is used to define the solid angle of the cone. *Steradian* is the name given to one unit solid angle. A *steradian is the solid angle subtended at the center of a sphere of one meter radius by an area of one square meter on its surface.* An increase of the area inscribed on a given sphere indicates a proportionate increase in the solid angle, and a total solid angle inscribes the total surface area of $4\pi r^2$. The total solid angle is then 4π steradians, in the same sense as the total plane angle is 2π radians. However, it is often convenient to think of solid angles that exceed 4π steradians, just as it is often convenient to think of plane angles that exceed 2π radians.

Elemental solid angles. In defining solid angles, areas inscribed on the surface of a specially located sphere were utilized. It is often desirable to express solid angles in terms of areas inscribed on very irregular surfaces. Since potatoes have such irregular shapes, they are ideal for visualizing general volumes and general surfaces. If, as in Fig. 3–2, a point O is chosen anywhere inside such a potato, an element of the skin area ds will subtend at O an element of solid angle $d\omega$. By definition, $d\omega = ds_n/r^2$, where r is the distance from O to the center of ds and ds_n is the area inscribed by this elemental solid angle on the surface of a sphere of radius r drawn about O as a center. When ds is sufficiently small, $ds_n = ds \cos \theta$, which can be written as $ds_n = \mathbf{a}_r \cdot d\mathbf{s}$ by defining the element of area on this closed surface as a vector $d\mathbf{s}$ directed along the outward drawn normal. The expression for the elemental solid angle then becomes

$$d\omega = \mathbf{a}_r \cdot \frac{d\mathbf{s}}{r^2}, \qquad (3\text{–}1)$$

Note that if this is integrated over the whole surface of the potato the result must be 4π:

$$\int_s \mathbf{a}_r \cdot \frac{d\mathbf{s}}{r^2} = 4\pi. \qquad (3\text{–}2)$$

An expression for the solid angle of a right circular cone in terms of its apex angle is often needed. This can be obtained by integrating Eq. (3–1) over the circular cap of the sphere shown in Fig. 3–3. Using spherical coordinates, the surface element is $(r\, d\theta)(r \sin\theta\, d\phi) = \mathbf{a}_r \cdot d\mathbf{s}$.

Fig. 3–1. The solid angle subtended by areas s_1, s_2 on two concentric spheres.
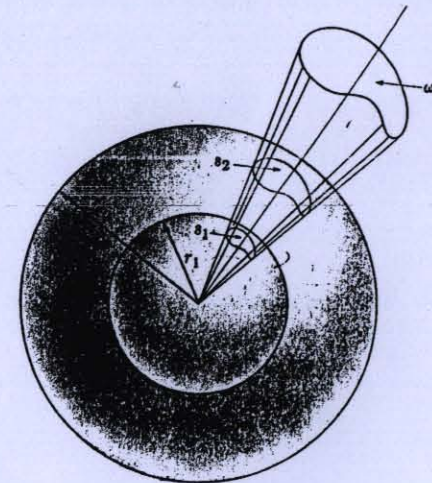

FIG. 3–2. An illustration of the elemental solid angle $d\omega = ds_n/r^2$ subtended by the area ds on the surface of a potato.
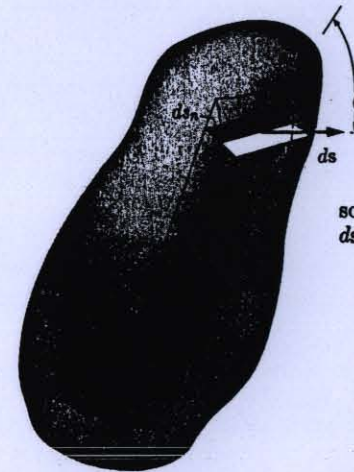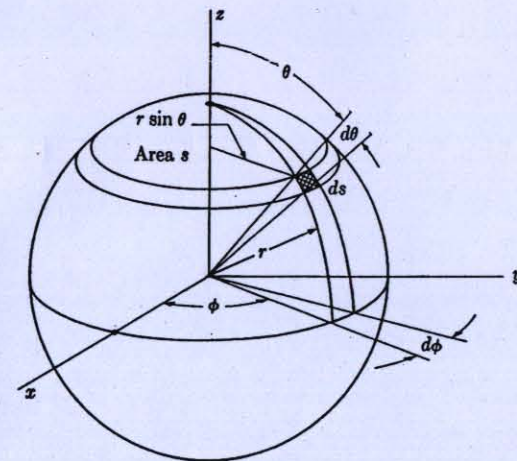

FIG. 3–3. An illustration showing how the solid angle of a right conical section is obtained from an integration of the elemental solid angle ds/r^2.

The significance of each of these parameters is explained below.

1. *Width of main beam* (or simply **beamwidth**). The main-beam beamwidth describes the sharpness of the main radiation region. It is generally taken to be the angular width of a pattern between the half-power, or -3 (dB), points. In electric-intensity plots it is the angular width between points that are $1/\sqrt{2}$ or 0.707 times the maximum intensity. Thus, the *H*-plane pattern in Fig. 11–4 has a 3 (dB) beamwidth equal to $(\phi_2 - \phi_1)$, and the *E*-plane pattern of the Hertzian dipole in Fig. 11–3(a) has a 3 (dB) beamwidth of 90°. Occasionally the angular width of the main beam between -10 (dB) points or between the first nulls is also of interest. Of course, the main beam must point in the direction where the antenna is designed to have its maximum radiation.

2. *Sidelobe levels.* Sidelobes of a directive (nonisotropic) pattern represent regions of unwanted radiation; they should have levels as low as possible. Generally, the levels of distant sidelobes are lower than the levels of those near the main beam. Hence, when one talks about the sidelobe level of an antenna pattern, one usually refers to the first (the nearest and highest) sidelobe. In modern radar applications, sidelobe levels of the order of minus 40 or more decibels are required. In practical applications the locations of the sidelobes are also of importance.

3. *Directivity.* The beamwidth of an antenna pattern specifies the sharpness of the main beam, but it does not provide us with any information about the rest of the pattern. For example, the sidelobes may be very high—an undesirable feature. A commonly used parameter to measure the overall ability of an antenna to direct radiated power in a given direction is *directive gain*, which may be defined in terms of radiation intensity. *Radiation intensity* is the time-average power per unit solid angle. The SI unit for radiation intensity is watt per steradian (W/sr). Since there are R^2 square meters of spherical surface area for each unit solid angle, radiation intensity, U, equals R^2 times the time-average power per unit area or R^2 times the magnitude of the time-average Poynting vector, $\mathscr{P}_{av}$:

$$U = R^2 \mathscr{P}_{av} \quad \text{(W/sr)}. \tag{11-32}$$

The total time-average power radiated is

$$P_r = \oint \mathscr{P}_{av} \cdot d\mathbf{s} = \oint U \, d\Omega \quad \text{(W)}, \tag{11-33}$$

where $d\Omega$ is the differential solid angle, $d\Omega = \sin\theta \, d\theta \, d\phi$. The *directive gain*, $G_D(\theta, \phi)$, of an antenna pattern is the ratio of the radiation intensity in the direction (θ, ϕ) to the average radiation intensity:

$$G_D(\theta, \phi) = \frac{U(\theta, \phi)}{P_r/4\pi} = \frac{4\pi U(\theta, \phi)}{\oint U \, d\Omega}. \tag{11-34}$$

Obviously, the directive gain of an isotropic or omnidirectional antenna (an antenna that radiates uniformly in all directions) is unity. However, an isotropic antenna does not exist in practice.

The maximum directive gain of an antenna is called the **directivity** of the antenna. It is the ratio of the maximum radiation intensity to the average radiation intensity and is usually denoted by D:

$U_{av} = \cfrac{\oint U \, d\Omega}{\left(\int d\Omega\right)}$

$= \cfrac{}{4\pi}$

$$\boxed{D = \frac{U_{max}}{U_{av}} = \frac{4\pi U_{max}}{P_r} \qquad \text{(Dimensionless)}.}$$ (11-35)

In terms of electric field intensity, D can be expressed as

$$\boxed{D = \frac{4\pi|E_{max}|^2}{\int_0^{2\pi} \int_0^{\pi} |E(\theta, \phi)|^2 \sin\theta \, d\theta \, d\phi} \qquad \text{(Dimensionless)}.}$$ (11-36)

Directivity is frequently expressed in decibels, referring to unity.

━━━━ **EXAMPLE 11-2** Find the directive gain and the directivity of a Hertzian dipole.

Solution For a Hertzian dipole the magnitude of the time-average Poynting vector is

$H_\phi = j \dfrac{I \, d\ell}{4\pi}\left(\dfrac{e^{-j\beta R}}{R}\right)\beta \sin\theta$ (11-19a)

$\mathscr{P}_{av} = \frac{1}{2}\mathscr{R}e\left[\mathbf{E} \times \mathbf{H}^*\right] = \frac{1}{2}|E_\theta||H_\phi|.$ (11-37)

Hence from Eqs. (11-19a, b) and (11-32),

$E_\theta = j \dfrac{I \, d\ell}{4\pi}\left(\dfrac{e^{-j\beta R}}{R}\right)\eta_0 \beta \sin\theta$ (11-19b)

$U = \dfrac{(I \, d\ell)^2}{32\pi^2}\eta_0\beta^2 \sin^2\theta. \;=\; R^2 \mathscr{P}_{av}$ (11-38)

The directive gain can be obtained from Eq. (11-34):

$$G_D(\theta, \phi) = \frac{4\pi \sin^2\theta}{\int_0^{2\pi} \int_0^{\pi} (\sin^2\theta) \sin\theta \, d\theta \, d\phi}$$

$$= \tfrac{3}{2}\sin^2\theta.$$

The directivity is the maximum value of $G_D(\theta, \phi)$:

$$D = G_D\left(\frac{\pi}{2}, \phi\right) = 1.5,$$

which corresponds to $10\log_{10} 1.5$ or 1.76 (dB).

We note that beamwidth, sidelobe levels, and directive gain are parameters of an antenna pattern; they do not convey information about the efficiency or the input impedance of the antenna. A measure of antenna efficiency is the power gain. The **power gain**, or simply the **gain**, G_P, of an antenna referred to an isotropic source is the ratio of its maximum radiation intensity to the radiation intensity of a lossless isotropic source with the same power input. The directive gain as defined in Eq. (11-34) is based on radiated power P_r. Because of ohmic power loss, P_ℓ, in the

antenna itself as well as in nearby lossy structures including the ground, P_r is less than the total input power P_i. We have

$$P_i = P_r + P_\ell. \tag{11-39}$$

The power gain of an antenna is then

$$G_p = \frac{U_{max}}{\left(\frac{P_i}{4\pi}\right)} \Rightarrow \boxed{G_P = \frac{4\pi U_{max}}{P_i} \quad \text{(Dimensionless).}} \tag{11-40}$$

$$\neq \quad \text{average input power}$$
$$\frac{\oint U_{in}\,d\Omega}{\int d\Omega}$$

The ratio of the gain to the directivity of an antenna is the **radiation efficiency**, η_r:

$$\boxed{\eta_r = \frac{G_P}{D} = \frac{P_r}{P_i} \quad \text{(Dimensionless).}} \tag{11-41}$$

Normally, the efficiency of well-constructed antennas is very close to 100%.

A useful measure of the amount of power radiated by an antenna is radiation resistance. The **radiation resistance** of an antenna is the value of a hypothetical resistance that would dissipate an amount of power equal to the radiated power P_r when the current in the resistance is equal to the maximum current along the antenna. Naturally, a high radiation resistance is a desirable property for an antenna.

EXAMPLE 11-3   Find the radiation resistance of a Hertzian dipole.

Solution   If we assume no ohmic losses, the time-average power radiated by a Hertzian dipole for an input time-harmonic current with an amplitude I is

$$P_r = \oint R^2 \mathcal{P}_{av}\,d\Omega \Rightarrow \quad P_r = \tfrac{1}{2}\int_0^{2\pi}\int_0^\pi \overbrace{E_\theta H_\phi^*}^{Re} R^2 \sin\theta\,d\theta\,d\phi. \tag{11-42}$$

$\ell\ell$

$\oint \vec{\mathcal{P}}_{av} \cdot d\vec{s}$
where S is a spherical surface

Using the far-zone fields in Eqs. (11-19a, b), we find

$$P_r = \frac{I^2(d\ell)^2}{32\pi^2}\,\eta_0\beta^2 \int_0^{2\pi}\int_0^\pi \sin^3\theta\,d\theta\,d\phi$$
$$= \frac{I^2(d\ell)^2}{12\pi}\,\eta_0\beta^2 = \frac{I^2}{2}\left[80\pi^2\left(\frac{d\ell}{\lambda}\right)^2\right]. \tag{11-43}$$

In this last expression we have used 120π for the intrinsic impedance of free space, η_0, and substituted $2\pi/\lambda$ for β.

Since the current along the short Hertzian dipole is uniform, we refer the power dissipated in the radiation resistance R_r to I. Equating $I^2 R_r/2$ to P_r, we obtain

$$\boxed{R_r = 80\pi^2\left(\frac{d\ell}{\lambda}\right)^2 \quad (\Omega).} \tag{11-44}$$

As an example, if $d\ell = 0.01\lambda$, R_r is only about 0.08 (Ω), an extremely small value. Hence a short dipole antenna is a poor radiator of electromagnetic power. However, it is erroneous to say without qualification that the radiation resistance of a dipole antenna increases as the square of its length because Eq. (11–44) holds only if $d\ell \ll \lambda$.

Radiation resistance may be quite different from the real part of the input impedance because the latter includes ohmic losses in the antenna structure itself as well as losses in the ground. The input impedance of a short dipole antenna has a large capacitive reactance, which makes it difficult to match and therefore difficult to feed power to the antenna efficiently.

EXAMPLE 11-4 Find the radiation efficiency of an isolated Hertzian dipole made of a metal wire of radius a, length $d\ell$ and conductivity σ.

Solution   Let I be the amplitude of the current in the wire dipole having a loss resistance R_ℓ. Then the ohmic power loss is

$$P_\ell = \tfrac{1}{2}I^2 R_\ell. \tag{11-45}$$

In terms of radiation resistance R_r, the radiated power is

$$P_r = \tfrac{1}{2}I^2 R_r. \tag{11-46}$$

From Eqs. (11–39) and (11–41) we have

$$\eta_r = \frac{P_r}{P_r + P_\ell} = \frac{R_r}{R_r + R_\ell}$$
$$= \frac{1}{1 + (R_\ell/R_r)}, \tag{11-47}$$

where R_r has been found in Eq. (11–44). The loss resistance R_ℓ of the metal wire can be expressed in terms of the surface resistance R_s:

$$R_\ell = R_s\!\left(\frac{d\ell}{2\pi a}\right), \tag{11-48}$$

where

$$R_s = \sqrt{\frac{\pi f \mu_0}{\sigma}} \tag{11-49}$$

as given in Eq. (9–26b). Using Eqs. (11–44) and (11–48) in Eq. (11–47), we obtain the radiation efficiency of an isolated Hertzian dipole:

$$\eta_r = \frac{1}{1 + \dfrac{R_s}{160\pi^3}\left(\dfrac{\lambda}{a}\right)\left(\dfrac{\lambda}{d\ell}\right)}. \tag{11-50}$$

Assume that $a = 1.8$ (mm), $d\ell = 2$ (m), operating frequency $f = 1.5$ (MHz), and σ (for copper) $= 5.80 \times 10^7$ (S/m). We find that

$$\lambda = \frac{c}{f} = \frac{3 \times 10^8}{1.5 \times 10^6} = 200 \quad (m),$$

$$R_s = \sqrt{\frac{\pi \times (1.50 \times 10^6) \times (4\pi 10^{-7})}{5.80 \times 10^7}} = 3.20 \times 10^{-4} \quad (\Omega),$$

$$R_\ell = 3.20 \times 10^{-4} \times \left(\frac{2}{2\pi 1.8 \times 10^{-3}}\right) = 0.057 \quad (\Omega),$$

$$R_r = 80\pi^2 \left(\frac{2}{200}\right)^2 = 0.079 \quad (\Omega),$$

and

$$\eta_r = \frac{0.079}{0.079 + 0.057} = 58\%,$$

which is very low. Equation (11–50) shows that smaller values of (a/λ) and $(d\ell/\lambda)$ lower the radiation efficiency.   ▬

11–4 Thin Linear Antennas

We have just indicated that a short dipole antenna is not a good radiator of electromagnetic power because of its low radiation resistance and low radiation efficiency. We now examine the radiation characteristics of a center-fed thin straight antenna having a length comparable to a wavelength, as shown in Fig. 11–5. Such an antenna is a *linear dipole antenna*. If the current distribution along the antenna is known, we can find its radiation field by integrating over the entire length of the antenna the radiation field due to an elemental dipole. The determination of the exact current distribution on such a seemingly simple geometrical configuration (a straight wire
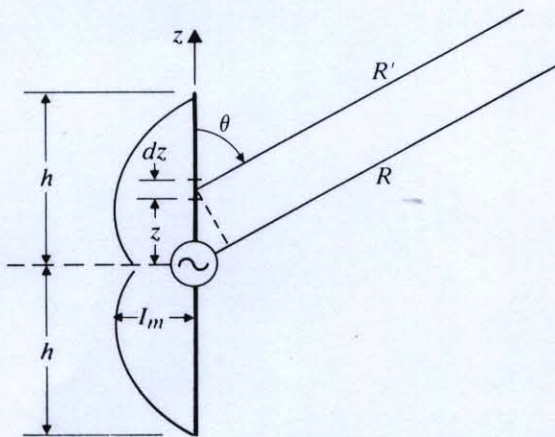

FIGURE 11–5
A center-fed linear dipole with sinusoidal current distribution.

of a finite radius) is, however, a very difficult boundary-value problem even if the wire is assumed to be perfectly conducting. The current must be zero at the ends of the wire where charges are deposited, and the tangential electric field due to all currents and charges must vanish at every point on the wire surface. An analytical formulation of the problem leads to an integral equation in which the current distribution along the antenna is the unknown function under the integral. Unfortunately, an exact solution of the integral equation does not exist. Various approximate solutions have been attempted. With the advent of high-speed digital computers, numerical solutions for current distributions and input impedances can be obtained for linear antennas of specific lengths and thicknesses. The ratio of the voltage and the current at the feed points is the input impedance. Both the solution procedure and the numerical results are quite involved, and we shall not delve into them in this book. For our purposes the knowledge of the exact current distribution on the linear antenna is not of prime importance; a good estimate will give us considerable useful information on the radiation characteristics of the antenna. We assume a sinusoidal current distribution on a very thin, straight dipole. Such a current distribution constitutes a kind of standing wave over the dipole and represents a good approximation.
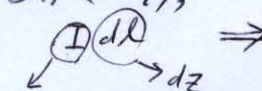
Since the dipole is center-driven, the currents on the two halves of the dipole are symmetrical and go to zero at the ends. We write the current phasor as

$$I(z) = I_m \sin \beta(h - |z|),$$

$$= \begin{cases} I_m \sin \beta(h - z), & z > 0, \\ I_m \sin \beta(h + z), & z < 0. \end{cases} \tag{11-51}$$

We are interested only in the far-zone fields. The far-field contribution from the differential current element $I\,dz$ is, from Eqs. (11-19a, b),

$$dE_\theta = \eta_0\, dH_\phi = j\frac{I\,dz}{4\pi}\left(\frac{e^{-j\beta R'}}{R'}\right)\eta_0\beta \sin\theta. \tag{11-52}$$

Now R' in Eq. (11-52) is slightly different from R measured to the origin of the spherical coordinates, which coincides with the center of the dipole. In the far zone, $R \gg h$,

$$R' = (R^2 + z^2 - 2Rz \cos\theta)^{1/2} \cong R - z\cos\theta. \tag{11-53}$$

The magnitude difference between $1/R'$ and $1/R$ is insignificant, but the approximate relation in Eq. (11-53) must be retained in the phase term. Using Eqs. (11-51) and (11-53) in Eq. (11-52) and integrating, we have

$$E_\theta = \eta_0 H_\phi$$

$$= j\frac{I_m\eta_0\beta \sin\theta}{4\pi R} e^{-j\beta R} \int_{-h}^{h} \sin\beta(h - |z|)e^{j\beta z \cos\theta}\, dz. \tag{11-54}$$

The integrand in Eq. (11-54) is the product of an even function of z, $\sin\beta(h - |z|)$, and

$$e^{j\beta z \cos\theta} = \cos(\beta z \cos\theta) + j\sin(\beta z \cos\theta),$$

where $\sin(\beta z \cos \theta)$ is an odd function of z. Integrating between symmetrical limits $-h$ and h, we find that only the part of the integrand containing the product $\sin \beta(h - |z|) \cos(\beta z \cos \theta)$ does not vanish. Equation (11–54) then reduces to

$$E_\theta = \eta_0 H_\phi = j\,\frac{I_m \eta_0 \beta \sin \theta}{2\pi R}\, e^{-j\beta R} \int_0^h \sin \beta(h - z) \cos(\beta z \cos \theta)\,dz$$

$$= \frac{j60 I_m}{R}\, e^{-j\beta R} F(\theta),$$

(11–55)

where

$$F(\theta) = \frac{\cos(\beta h \cos \theta) - \cos \beta h}{\sin \theta}.$$

(11–56)

The factor $|F(\theta)|$ is the E-plane *pattern function* of a linear dipole antenna. It describes the radiation pattern or the variation of the normalized far field, $|E_\theta|$, versus the angle θ. The exact shape of the radiation pattern represented by $|F(\theta)|$ in Eq. (11–56) depends on the value of $\beta h = 2\pi h/\lambda$ and can be quite different for different antenna lengths. The radiation pattern, however, is always symmetrical with respect to the $\theta = \pi/2$ plane. Figure 11–6 shows the E-plane patterns for four different dipole lengths measured in terms of wavelength: $2h/\lambda = \frac{1}{2}, 1, \frac{3}{2}$ and 2. The H-plane patterns are circles inasmuch as $F(\theta)$ is independent of ϕ. From the patterns in Fig. 11–6 we see that the direction of maximum radiation tends to shift away from the $\theta = 90°$ plane when the dipole length approaches $3\lambda/2$. For $2h = 2\lambda$ there is no radiation in the $\theta = 90°$ plane.

(a) $2h/\lambda = 1/2$.

(b) $2h/\lambda = 1$.

(c) $2h/\lambda = 3/2$.

(d) $2h/\lambda = 2$.
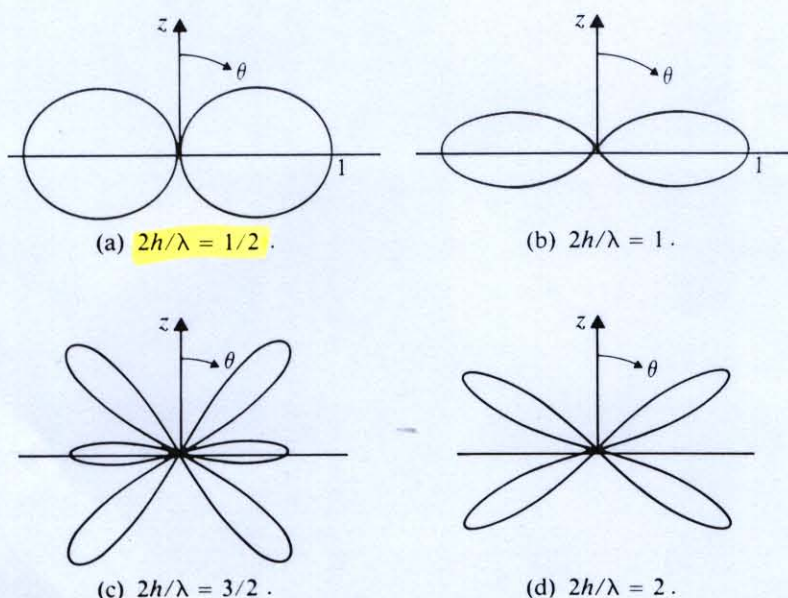
FIGURE 11–6
E-plane radiation patterns for center-fed dipole antennas.

11-4.1   THE HALF-WAVE DIPOLE

The half-wave dipole having a length $2h = \lambda/2$ is of particular practical importance because of its desirable pattern and impedance characteristics. We shall now examine its properties in more detail.

For a half-wave dipole, $\beta h = 2\pi h/\lambda = \pi/2$, the pattern function in Eq. (11-56) becomes

$$F(\theta) = \frac{\cos\left[(\pi/2)\cos\theta\right]}{\sin\theta}. \tag{11-57}$$

This function has a maximum equal to unity at $\theta = 90°$ and has nulls at $\theta = 0°$ and $180°$. The corresponding E-plane radiation pattern is sketched in Fig. 11-6(a). The far-zone field phasors are, from Eq. (11-55),

$$E_\theta = \frac{j60I_m}{R} e^{-j\beta R} \left\{ \frac{\cos\left[(\pi/2)\cos\theta\right]}{\sin\theta} \right\} \tag{11-58}$$

and

$$H_\phi = \frac{jI_m}{2\pi R} e^{-j\beta R} \left\{ \frac{\cos\left[(\pi/2)\cos\theta\right]}{\sin\theta} \right\}. \tag{11-59}$$

The magnitude of the time-average Poynting vector is

$$\mathscr{P}_{av} = \frac{1}{2} E_\theta H_\phi^* = \frac{15I_m^2}{\pi R^2} \left\{ \frac{\cos\left[(\pi/2)\cos\theta\right]}{\sin\theta} \right\}^2. \tag{11-60}$$

The total power radiated by a half-wave dipole is obtained by integrating $\mathscr{P}_{av}$ over the surface of a great sphere:

$$\oint_S \mathscr{P}_{av} \cdot d\vec{s} = P_r = \int_0^{2\pi} \int_0^\pi \mathscr{P}_{av} R^2 \sin\theta \, d\theta \, d\phi$$

$$= 30I_m^2 \int_0^\pi \frac{\cos^2\left[(\pi/2)\cos\theta\right]}{\sin\theta} \, d\theta. \tag{11-61}$$

The integral in Eq. (11-61) can be evaluated numerically to give a value 1.218. Hence

$$P_r = 36.54 I_m^2 \quad \text{(W)}, \tag{11-62}$$

from which we obtain the radiation resistance of a free-standing half-wave dipole:

$$R_r = \frac{2P_r}{I_m^2} = 73.1 \quad (\Omega). \tag{11-63}$$

Neglecting losses, we find that the input resistance of a thin half-wave dipole equals 73.1 (Ω) and that the input reactance is a small positive number that can be made to vanish when the dipole length is adjusted to be slightly shorter than $\lambda/2$. (As we have indicated before, the actual calculation of the input impedance is tedious and is beyond the scope of this book.)

The directivity of a half-wave dipole can be found by using Eq. (11–35). We have, from Eqs. (11–32) and (11–60),

$$\mathcal{P}_{av} = \frac{15 I_m^2}{\pi R^2} \left\{ \frac{\cos\left[(\pi/2)\cos\theta\right]}{\sin\theta} \right\}^2 \Rightarrow U_{max} = R^2 \mathcal{P}_{av}(90°) = \frac{15}{\pi} I_m^2 \tag{11–64}$$

and

$$D = \frac{4\pi U_{max}}{P_r} = \frac{60}{36.54} = 1.64, \tag{11–65}$$

which corresponds to $10 \log_{10} 1.64$ or 2.15 (dB) referring to an omnidirectional radiator.

The half-power beamwidth of the radiation pattern is the angle between the two solutions of the equation

$$\frac{\cos\left[(\pi/2)\cos\theta\right]}{\sin\theta} = \frac{1}{\sqrt{2}}, \qquad 0 < \theta < \pi,$$

which can be solved either numerically or graphically to give a beamwidth of 78°. Thus a half-wave dipole is only slightly more directive than a short Hertzian dipole that has a directivity of 1.76 (dB) and a beamwidth of 90°.

___ EXAMPLE 11–5   A thin quarter-wavelength vertical antenna over a perfectly conducting ground is excited by a sinusoidal source at its base. Find its radiation pattern, radiation resistance, and directivity.

Solution   Since current is charge in motion, we can use the method of images discussed in Section 4–4 and replace the conducting ground by the image of the vertical antenna. A little thought will convince us that the image of a vertical antenna carrying a current I is another vertical antenna. The image antenna has the same length, is equidistant from the ground, and carries the same current in the *same direction* as
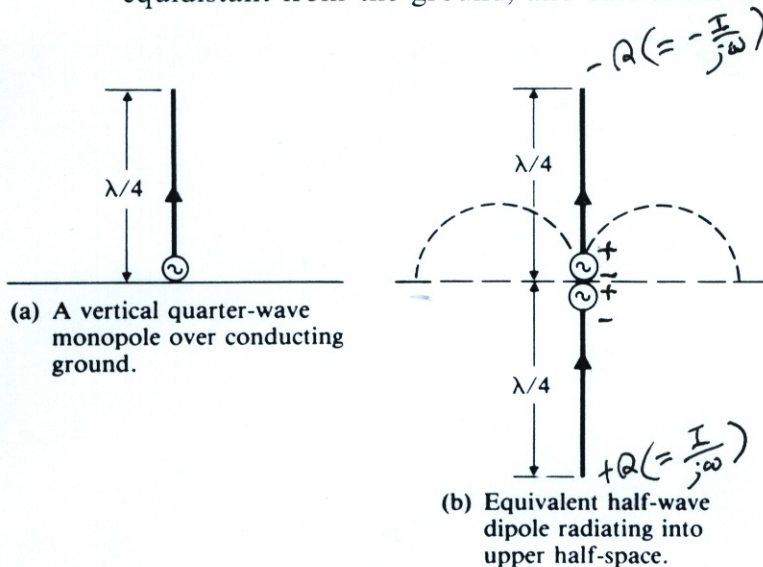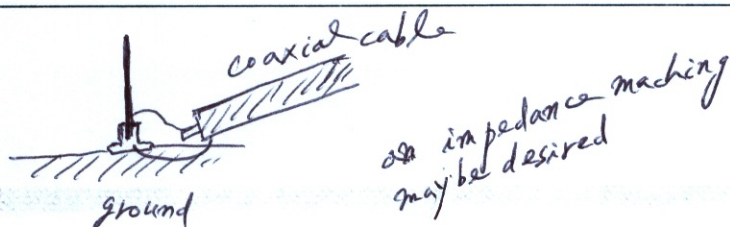

(a) A vertical quarter-wave monopole over conducting ground.

(b) Equivalent half-wave dipole radiating into upper half-space.

FIGURE 11–7
Quarter-wave monopole over a conducting ground and its equivalent half-wave dipole.

the original antenna. The electromagnetic field *in the upper half-space* due to the quarter-wave vertical antenna in Fig. 11–7(a) is, then, the same as that of the half-wave antenna in Fig. 11–7(b). The pattern function in Eq. (11—57) applies here for $0 \le \theta \le \pi/2$, and the radiation pattern drawn in dashed lines in Fig. 11–7(b) is the upper half of that in Fig. 11–6(a).

The magnitude of the time-average Poynting vector, $\mathscr{P}_{av}$, in Eq. (11–60), holds for $0 \le \theta \le \pi/2$. Inasmuch as the quarter-wave antenna (a **monopole**) radiates only into the upper half-space, its total radiated power is only one-half that given in Eq. (11–62):

$$P_r = 18.27 I_m^2 \quad (\text{W}).$$

Consequently, the radiation resistance is

$$R_r = \frac{2P_r}{I_m^2} = 36.54 \quad (\Omega), \tag{11–66}$$

which is one-half of the radiation resistance of a half-wave antenna in free-space.

To calculate directivity, we note that although the maximum radiation intensity U_{max} remains the same as that given in Eq. (11–64), the average radiation intensity is now $P_r/2\pi$. Thus,

$$D = \frac{U_{max}}{U_{av}} = \frac{U_{max}}{(P_r/2\pi)} = 1.64, \tag{11–67}$$

the same since P_r reduced half while $4\pi \to 2\pi$.

which is the same as the directivity of a half-wave antenna.

11-4.2   EFFECTIVE ANTENNA LENGTH

For thin linear antennas with a given current distribution it is sometimes convenient to define a quantity called the **effective length**, to which the far-zone field is proportional. Let us refer to the dipole antenna in Fig. 11–5 and assume a general phasor current distribution $I(z)$. The far-zone field is then, from Eq. (11–54),

$$E_\theta = \eta_0 H_\phi = \frac{j30}{R} \beta e^{-j\beta R} \left\{ \sin\theta \int_{-h}^{h} I(z) e^{j\beta z \cos\theta} \, dz \right\}. \tag{11–68}$$

Let $I(0)$ be the input current at the feed point of the antenna. We write Eq. (11–68) as

$$E_\theta = \eta_0 H_\phi = \frac{j30 I(0)}{R} \beta e^{-j\beta R} \ell_e(\theta), \tag{11–69}$$

where

$$\ell_e(\theta) = \frac{\sin\theta}{I(0)} \int_{-h}^{h} I(z) e^{j\beta z \cos\theta} \, dz \tag{11–70}$$

is the **effective length** of the transmitting antenna. (We will discuss the effective length of a receiving antenna presently.) As we see from Eq. (11–69), ℓ_e measures the effectiveness of the antenna as a radiator, and for a given current distribution the far-zone field is proportional to ℓ_e, which contains all the information about the directional properties of the antenna. In most practical situations the important value of the

effective length is that at $\theta = \pi/2$, where

$$\ell_e = \frac{1}{I(0)} \int_{-h}^{h} I(z)\,dz \qquad \text{(m)}.$$
(11–71)

Equation (11–71) indicates that ℓ_e is the length of an equivalent linear antenna with a uniform current $I(0)$ such that it radiates the same far-zone field in the $\theta = \pi/2$ plane.

EXAMPLE 11–6   Assume a sinusoidal current distribution on a center-fed, thin, straight half-wave dipole. Find its effective length. What is its maximum value?

Solution   For the assumed sinusoidal current distribution we use Eq. (11–51) for $I(z)$ and substitute it in Eq. (11–70), where $I(0) = I_m$ and $h = \lambda/4$. We have

$$\ell_e(\theta) = \sin\theta \int_{-\lambda/4}^{\lambda/4} \sin\beta\left(\frac{\lambda}{4} - |z|\right) e^{j\beta z\cos\theta}\,dz.$$
(11–72)

The above integral has been evaluated in Eq. (11–56). Thus,

$$\ell_e(\theta) = \frac{2}{\beta}\left[\frac{\cos\left(\dfrac{\pi}{2}\cos\theta\right)}{\sin\theta}\right].$$
(11–73)

The maximum value of $\ell_e(\theta)$ is at $\theta = \pi/2$, where the effective length is

$$\ell_e\left(\frac{\pi}{2}\right) = \frac{2}{\beta} = \frac{\lambda}{\pi}.$$
(11–74)

We note from Eq. (11–74) that the maximum effective length of a half-wave dipole is less than its physical length, $\lambda/2$.

A careful examination of Eq. (11–71) reveals a potential anomaly in the appearance of $I(0)$ in the denominator. When the half-length of a dipole is greater than $\lambda/4$ and approaches $\lambda/2$, $I(0)$ would be progressively less than I_m, which would not occur at $z = 0$. This could make ℓ_e much greater than $2h$. Thus the definition of effective length as given in Eqs. (11–70) and (11–71) is meaningful only for relatively short antennas that have a current maximum at the feed point.

The effective length of a receiving linear antenna is defined as the ratio of the open-circuit voltage V_{oc} induced at the antenna terminals and the electric field intensity $E_i = |\mathbf{E}_i|$ at the antenna that induces it:

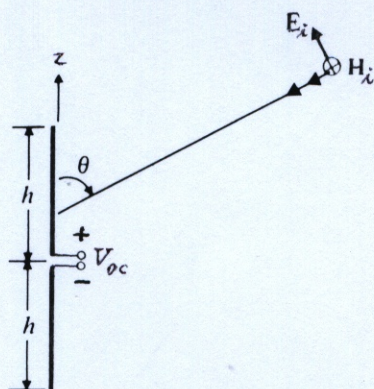$$\ell_e(\theta) = -\frac{V_{oc}}{E_i},$$
(11–75)

FIGURE 11-8
A linear antenna in the receiving mode.

where the negative sign is to conform with the convention that the electric potential increases in a direction opposite to that of the electric field. The situation is illustrated in Fig. 11–8. We will assume that $\mathbf{E}_i$ lies in the plane of incidence, since the component of $\mathbf{E}_i$ normal to the antenna does not induce a voltage across the antenna terminals. Obviously, the open-circuit voltage V_{oc} depends on E_i, θ, and βh in a complicated way. It is possible to use a reciprocity theorem to prove formally that *the effective length of an antenna for receiving is the same as that for transmitting* [14].[†] In Section 11–6 we shall prove that both the impedance and the directional pattern of an isolated antenna in the receiving mode are the same as those of the antenna in the transmitting mode. We may also conclude the equality of the effective lengths operating under these two modes.

If the incoming electric field $\mathbf{E}_i$ is not parallel to the dipole, there is a polarization mismatch, and the magnitude of the open-circuit voltage will be

$$|V_{oc}| = |\boldsymbol{\ell}_e \cdot \mathbf{E}_i|, \tag{11–76}$$

where $\boldsymbol{\ell}_e$ denotes the vector effective length. Obviously, $|V_{oc}|$ will be maximum when $\mathbf{E}_i$ is parallel to the dipole and will be zero if $\mathbf{E}_i$ is perpendicular to the dipole.

11–5 Antenna Arrays

Antenna arrays are groups of similar antennas arranged in various configurations (straight lines, circles, triangles, and so on) with proper amplitude and phase relations to give certain desired radiation characteristics. Frequently, the radiation characteristics of importance are the direction and width of the main beam, sidelobe levels, and/or directivity. In this section we examine the basic theories and characteristics of linear antenna arrays (radiating elements arranged along a straight line). The electromagnetic field of an array is the vector superposition of the fields produced by

---

[†] Bracketed numbers refer to the literature listed in the reference section at the end of this chapter.

the individual antenna elements. We first consider the simplest case of two-element arrays. After some experience has been gained with them, we consider the basic properties of uniform linear arrays made up of many identical elements.

11–5.1   TWO-ELEMENT ARRAYS

The simplest array is one consisting of two identical radiating elements (antennas) spaced a distance apart. This is illustrated in Fig. 11-9. For simplicity, let us assume that the far-zone electric field of the individual antennas be in the θ-direction and that the antennas are lined along the x-axis. The antennas are excited with a current of the same magnitude, but the phase in antenna 1 leads that in antenna 0 by an angle ξ. We have

$$E_0 = E_m F(\theta, \phi) \frac{e^{-j\beta R_0}}{R_0}, \tag{11-77}$$

$$E_1 = E_m F(\theta, \phi) \frac{e^{j\xi}e^{-j\beta R_1}}{R_1}, \tag{11-78}$$

where $F(\theta, \phi)$ is the pattern function of the individual antennas, and E_m is an amplitude function. The electric field of the two-element array is the sum of E_0 and E_1. Hence,

since the E-fields are assumed to have $\vec{a}_\theta$ components only.

$$E = E_0 + E_1 = E_m F(\theta, \phi) \left[\frac{e^{-j\beta R_0}}{R_0} + \frac{e^{j\xi}e^{-j\beta R_1}}{R_1} \right]. \tag{11-79}$$

In the far zone, $R_0 \gg d/2$, and the factor $1/R_1$ in the magnitude may be replaced approximately by $1/R_0$. However, a small difference between R_0 and R_1 in the exponents may lead to a significant phase difference, and a better approximation must be used. Because the lines joining the field point P and the two antennas are nearly parallel, we may write

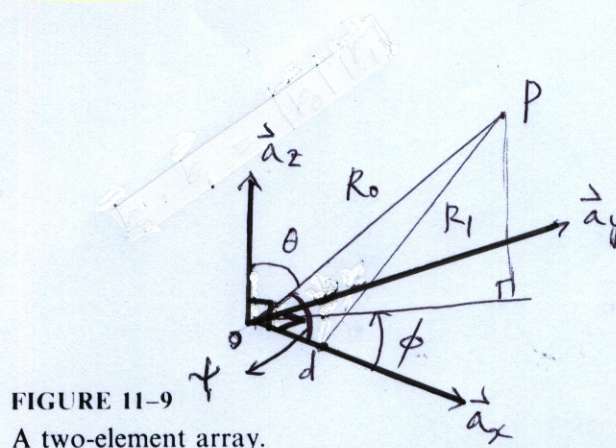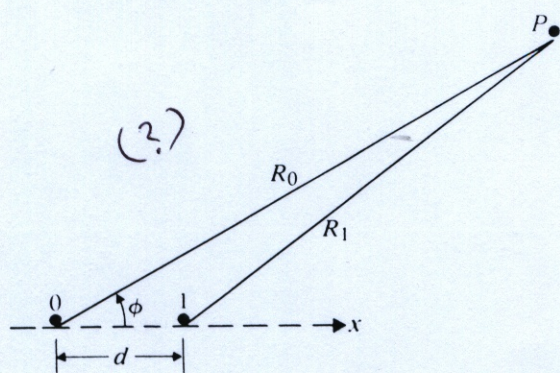$$R_1 \cong R_0 - d \sin \theta \cos \phi. \tag{11-80}$$

(?)

FIGURE 11–9
A two-element array.

$$\cos \psi = \sin \theta \cos \phi$$

$$\vec{R}_0 \cdot \vec{a}_x = |\vec{R}_0| \cos \psi$$

Substitution of Eq. (11-80) in Eq. (11-79) yields

$$E = E_m \frac{F(\theta, \phi)}{R_0} e^{-j\beta R_0} [1 + e^{j\beta d \sin\theta \cos\phi} e^{j\xi}]$$

$$= E_m \frac{F(\theta, \phi)}{R_0} e^{-j\beta R_0} e^{j\psi/2} \left(2 \cos \frac{\psi}{2}\right), \qquad (11\text{-}81)$$

where

$$\psi = \beta d \sin\theta \cos\phi + \xi. \qquad (11\text{-}82)$$

The magnitude of the electric field of the array is

$$|E| = \frac{2E_m}{R_0} |F(\theta, \phi)| \left|\cos \frac{\psi}{2}\right|, \qquad (11\text{-}83)$$

where $|F(\theta, \phi)|$ may be called the **element factor**, and $|\cos(\psi/2)|$ the normalized **array factor**. The element factor is the magnitude of the pattern function of the individual radiating elements, and the array factor depends on array geometry as well as on the relative amplitudes and phases of the excitations in the elements. (In this particular case the excitation amplitudes are equal.) The array factor is that of an array of *isotropic* elements, the directional property of the elements having been accounted for by the element factor. From Eq. (11-83) we may conclude that **the pattern function of an array of identical elements is described by the product of the element factor and the array factor**. This property is called the **principle of pattern multiplication**.

For an array of two parallel z-directed half-wave dipoles the magnitude of the total electric field is, from Eqs. (11-57) and (11-83),

$$|E| = \frac{2E_m}{R_0} \left|\frac{\cos\left[(\pi/2)\cos\theta\right]}{\sin\theta}\right| \left|\cos \frac{\psi}{2}\right|. \qquad (11\text{-}84)$$

Since ψ is also a function of θ, we see that the pattern in an E-plane is not the same as that of a single dipole, except when $\phi = \pm\pi/2$. In the H-plane, $\theta = \pi/2$, and the pattern is determined entirely by the array factor $|\cos(\psi/2)|$.

━━━ **EXAMPLE 11-7** Plot the H-plane radiation patterns of two parallel dipoles for the following two cases: (a) $d = \lambda/2$, $\xi = 0$; (b) $d = \lambda/4$, $\xi = -\pi/2$.
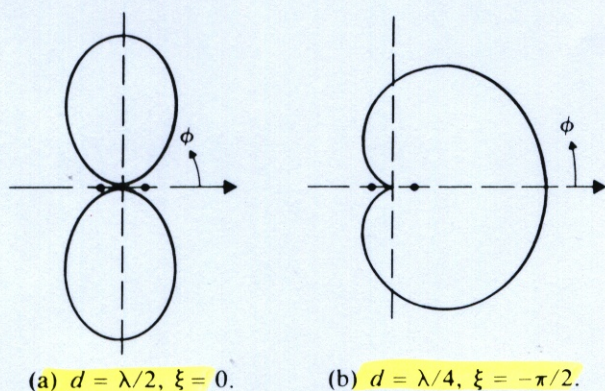
Solution Let the dipoles be z-directed and placed along the x-axis, as shown in Fig. 11-9. In the H-plane ($\theta = \pi/2$), each dipole is omnidirectional, and the normalized pattern function is equal to the normalized array factor $|A(\phi)|$. Thus

$$|A(\phi)| = \left|\cos \frac{\psi}{2}\right| = \left|\cos \frac{1}{2}(\beta d \cos\phi + \xi)\right|.$$

a) $d = \lambda/2$ ($\beta d = \pi$), $\xi = 0$:

$$|A(\phi)| = \left|\cos\left(\frac{\pi}{2}\cos\phi\right)\right|. \qquad (11\text{-}85a)$$

FIGURE 11–10
H-plane radiation patterns of two-element parallel dipole array.

(a) $d = \lambda/2$, $\xi = 0$.   (b) $d = \lambda/4$, $\xi = -\pi/2$.

The pattern has its maximum at $\phi_0 = \pm\pi/2$—that is, in the broadside direction. This is a type of **broadside array**. Figure 11–10(a) shows this broadside pattern. Since the excitations in the two dipoles are in phase, their electric fields add in the broadside directions, $\phi = \pm\pi/2$. At $\phi = 0$ and π the electric fields cancel each other because the $\lambda/2$ separation leads to a phase difference of 180°.

b) $d = \lambda/4$ ($\beta d = \pi/2$), $\xi = -\pi/2$:

$$|A(\phi)| = \left|\cos\frac{\pi}{4}(\cos\phi - 1)\right|, \qquad (11\text{–}85b)$$

which has a maximum at $\phi_0 = 0$ and vanishes at $\phi = \pi$. The pattern maximum is now in a direction *along* the line of the array, and the two dipoles constitute an **endfire array**. Figure 11–10(b) shows this endfire pattern. In this case the phase in the right-hand dipole *lags* by $\pi/2$, which exactly compensates for the fact that its electric field arrives in the $\phi = 0$ direction a quarter of a cycle *earlier* than the electric field of the left-hand dipole. As a consequence, the electric fields add in the $\phi = 0$ direction. In the $\phi = \pi$ direction, the $\pi/2$ phase lag in the right-hand dipole plus the quarter-cycle delay results in a complete cancellation of the fields.

EXAMPLE 11–8   Discuss the radiation pattern of a linear array of the three isotropic sources spaced $\lambda/2$ apart. The excitations in the sources are in-phase and have amplitude ratios 1:2:1.

(a) Three-element binomial array.

(b) Two displaced two-element arrays.
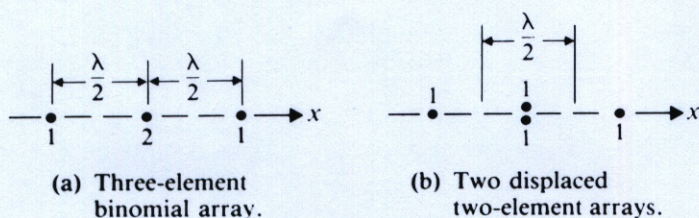
FIGURE 11–11
A three-element array and its equivalent pair of displaced two-element arrays.
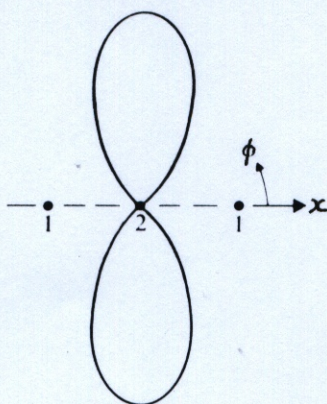
FIGURE 11–12
Radiation pattern of three-element broadside binomial array.

Solution   This three-source array is equivalent to two two-element arrays displaced $\lambda/2$ from each other as depicted in Fig. 11–11. Each two-element array can be considered as as a radiating source with an element factor as given by Eq. (11–85a) and an array factor, which is also given by the same equation. By the principle of pattern multiplication we obtain

$$|E| = \frac{4E_m}{R_0}\left|\cos\left(\frac{\pi}{2}\cos\phi\right)\right|^2. \qquad \theta = \frac{\pi}{2} \qquad (11\text{–}86)$$

The radiation pattern represented by the pattern function $|\cos[(\pi/2)\cos\phi]|^2$ is sketched in Fig. 11–12. Compared to the pattern of the uniform two-element array in Fig. 11–10(a), this three-element broadside pattern is sharper (more directive). Both patterns have no sidelobes.

The three-element broadside array is a special case of a class of *sidelobeless* arrays called **binomial arrays**. In a binomial array of N elements the excitation amplitudes vary according to the coefficients of a binomial expansion $\binom{N-1}{n}$, $n = 0, 1, 2, \ldots, N - 1$. For $N = 3$ the relative excitation amplitudes are $\binom{2}{0} = 1$, $\binom{2}{1} = 2$ and $\binom{2}{2} = 1$, as in Example 11–8. To obtain a directive pattern without sidelobes, d in a binomial array is normally restricted to be $\lambda/2$. The feature of no sidelobes in the array pattern of a binomial array is accompanied by a wider beamwidth and a lower directivity compared to those of a uniform array with the same number of elements.

11–5.2   GENERAL UNIFORM LINEAR ARRAYS

We now consider an array of identical antennas equally spaced along a straight line. The antennas are fed with currents of equal magnitude and have a uniform progressive phase shift along the line. Such an array is called a **uniform linear array**. An example is shown in Fig. 11–13, where N antenna elements are aligned along the x-axis. Since the antenna elements are identical, the array pattern function is the product of the element factor and the array factor. Our attention here will be concentrated on the
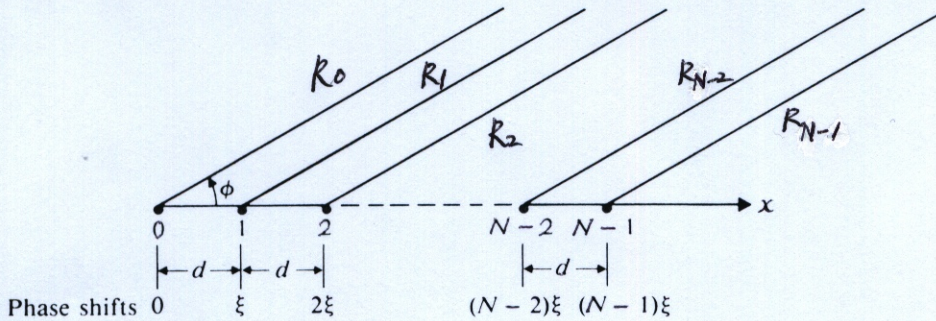
FIGURE 11–13
A general uniform linear array.

---

manner in which the array factor depends on the parameter βd $(= 2\pi d/\lambda)$ and the progressive phase shift ξ between neighboring elements. The normalized array factor in the xy-plane is

$$\theta = \frac{\pi}{2}$$

$$|A(\psi)| = \frac{1}{N}|1 + e^{j\psi} + e^{j2\psi} + \cdots + e^{j(N-1)\psi}|, \tag{11-87}$$

where

$$\psi = \beta d \cos \phi + \xi. \tag{11-88}$$

The polynomial on the right side of Eq. (11–87) is a geometric progression and can be summed up in a closed form:

$$|A(\psi)| = \frac{1}{N}\left|\frac{1 - e^{jN\psi}}{1 - e^{j\psi}}\right| = \frac{1}{N}\left|\frac{e^{jN\psi/2}(e^{-jN\psi/2} - e^{jN\psi/2})}{e^{j\psi/2}(e^{-j\psi/2} - e^{j\psi/2})}\right|$$

or

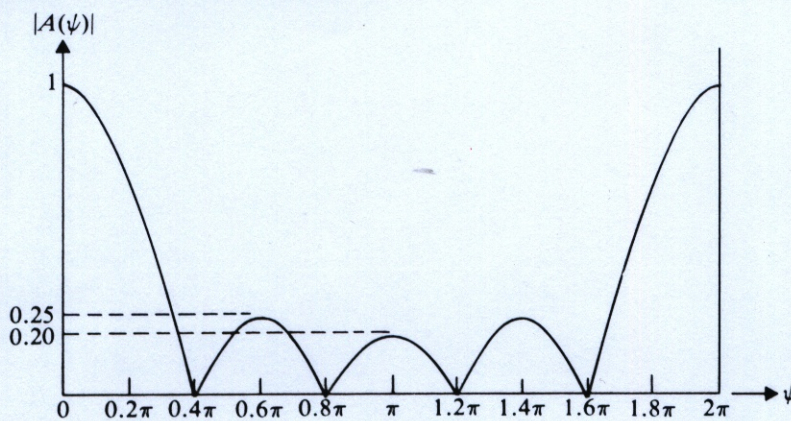$$\boxed{|A(\psi)| = \frac{1}{N}\left|\frac{\sin(N\psi/2)}{\sin(\psi/2)}\right|} \quad \text{(Dimensionless)}. \tag{11-89}$$

FIGURE 11–14
Normalized array factor of a five-element uniform linear array.

$$\langle \text{proof of } (11\text{-}89) \rangle$$

$$\theta = \frac{\pi}{2}, \quad E_k = E_m F\left(\frac{\pi}{2}, \phi\right)\frac{e^{-j\beta R_k}e^{jk\xi}}{R_k}, \quad R_k = R_k - d\cos\phi$$
$$= R_0 - kd\cos\phi$$

$$\Rightarrow E\left(k, \frac{\pi}{2}, \phi\right) = \sum_{k=0}^{N-1} E_k \simeq \frac{E_m F\left(\frac{\pi}{2}, \phi\right)}{R_0}\sum_{k=0}^{N-1} e^{j\beta R_0} e^{jk\psi}$$

$$\text{since } (N-1)d \ll R_0$$

This is the general expression of the normalized array factor for a uniform linear array. Figure 11–14 is a sketch of the normalized array factor for a five-element array. The actual radiation pattern as a function of ϕ depends on the values of βd and ξ (see Problem P.11–17). As ϕ varies from 0 to 2π, the value of ψ changes from $\beta d + \xi$ to $-\beta d + \xi$, covering a range of $2\beta d$ or $4\pi d/\lambda$. This defines the **visible range** of the radiation pattern.

We may derive several significant properties from $|A(\psi)|$ as given in Eq. (11–89).

1. *Main-beam direction.* The maximum value occurs when $\psi = 0$ or when

$$\beta d \cos \phi_0 + \xi = 0,$$

which leads to

$$\cos \phi_0 = -\frac{\xi}{\beta d}. \tag{11–90}$$

Two special cases are of particular importance.

a) *Broadside array.* For a broadside array, maximum radiation occurs at a direction perpendicular to the line of the array—that is, at $\phi_0 = \pm\pi/2$. This requires $\xi = 0$, which means that all the elements in a linear broadside array should be excited in phase, as was the case in Example 11–7(a). (*Fig. 11–10 (a)*)

b) *Endfire array.* For an endfire array, maximum radiation occurs at $\phi_0 = 0$. Equation (11–90) gives

$$\xi = -\beta d \cos \phi_0 = -\beta d.$$

We note that this condition is satisfied by the two-element array in Example 11–7(b). (*Fig. 11–10 (b)*)

2. *Null locations.* The array pattern has nulls when $|A(\phi)| = 0$ or when

$$\frac{N\psi}{2} = \pm k\pi, \qquad k = 1, 2, 3, \ldots. \tag{11–91}$$

It is obvious that the corresponding null locations in ϕ are different for broadside and endfire arrays because of the different values of ξ implicit in ψ.

3. *Width of main beam.* The angular width of the main beam between the first nulls can be determined approximately for large N. Let ψ_{01} denote the values of ψ at the first nulls:

$$\frac{N\psi_{01}}{2} = \pm\pi \qquad \text{or} \qquad \psi_{01} = \pm\frac{2\pi}{N}.$$

In order to see how ψ_{01} converts to an angle between the first nulls in ϕ, we need to know the direction of the main beam.

$(+\xi) = 0$

a) *Broadside array* $(\xi = 0, \phi_0 = \pi/2)$. For a broadside array, $\psi = \beta d \cos\phi$. If the first null occurs at ϕ_{01}, then the width of the main beam between the first nulls is $2\Delta\phi = 2(\phi_{01} - \phi_0)$. At ϕ_{01} we have

$$\cos \phi_{01} = \cos(\phi_0 + \Delta\phi) = \frac{\psi_{01}}{\beta d},$$

which, for $\phi_0 = \pi/2$, gives

$$\psi = \beta d \cos \phi \Rightarrow \cos \phi_{01} = \cos(\phi_0 + \Delta\phi)$$
$$= \psi_{01}/\beta d$$

$$\cos\left(\frac{\pi}{2} + \Delta\phi\right) = -\sin\Delta\phi = -\frac{2\pi}{N\beta d}$$

$$\begin{cases} \phi_0 = \pi/2 \\ \psi_{01} = \pm 2\pi/N \end{cases}$$

or

$$\Delta\phi = \sin^{-1}\left(\frac{\lambda}{Nd}\right) \cong \frac{\lambda}{Nd}. \tag{11-92}$$

The last approximation is obtained when $Nd \gg \lambda$. Equation (11-92) leads to a useful rule of thumb that the width of the main beam (in radians) of a long uniform broadside array is approximately *twice* the reciprocal of the array length in wavelengths.

b) *Endfire array* $(\xi = -\beta d, \phi_0 = 0)$. For an endfire array, $\psi = \beta d(\cos\phi - 1)$, and

$$\cos\phi_{01} - 1 = \frac{\psi_{01}}{\beta d} = -\frac{2\pi}{N\beta d} = -\frac{\lambda}{Nd}.$$

But $\cos\phi_{01} = \cos\Delta\phi \cong 1 - (\Delta\phi)^2/2$ for small $\Delta\phi$. Thus,

$$\frac{(\Delta\phi)^2}{2} \cong \frac{\lambda}{Nd}$$

or

$$\Delta\phi \cong \sqrt{\frac{2\lambda}{Nd}}. \tag{11-93}$$

Comparing Eq. (11-93) with Eq. (11-92), we may conclude that the width of the main beam of a uniform endfire array is greater than that of a uniform broadside array of the same length (because $Nd > \lambda/2$).

4. *Sidelobe locations.* Sidelobes are minor maxima that occur approximately when the numerator on the right side of Eq. (11-89) is a maximum—that is, when $|\sin(N\psi/2)| = 1$ or when

for large N

$$\frac{N\psi}{2} = \pm(2m + 1)\frac{\pi}{2}, \qquad m = 1, 2, 3, \ldots. \tag{11-94}$$

The first sidelobes occur when

$$\frac{N\psi}{2} = \pm\frac{3}{2}\pi, \qquad (m = 1). \tag{11-95}$$

Note that $N\psi/2 = \pm\pi/2$ $(m = 0)$ does not represent locations of sidelobes because they are still within the main-lobe region.

5. *First sidelobe level.* An important characteristic of the radiation pattern of an array is the level of the first sidelobes compared to that of the main beam, since the former is usually the highest of all sidelobes. All sidelobes should be kept as low as possible in order that most of the radiated power be concentrated in the main-beam direction and not be diverted to sidelobe regions. Substituting Eq.

(11–95) in Eq. (11–89), we find the amplitude of the first sidelobes to be

$$\frac{1}{N}\left|\frac{1}{\sin(3\pi/2N)}\right| \cong \frac{1}{N}\left|\frac{1}{3\pi/2N}\right| = \frac{2}{3\pi} = 0.212$$

for large N. In logarithmic terms the first sidelobes of a uniform linear antenna array of many elements are $20 \log_{10}(1/0.212)$ or 13.5 (dB) down from the principal maximum. This number is almost independent of N as long as N is large.

One way to reduce the sidelobe level in the radiation pattern of a linear array is to taper the current distribution in the array elements—that is, to make the excitation amplitudes in the elements in the center portion of an array higher than those in the end elements. This method is illustrated in the following example.

EXAMPLE 11–9 Find the array factor and plot the normalized radiation pattern of a broadside array of five isotropic elements spaced $\lambda/2$ apart and having excitation amplitude ratios 1:2:3:2:1. Compare the first sidelobe level with that of a five-element uniform array.

Solution The normalized array factor of the five-element tapered array is

$$|A(\psi)| = \tfrac{1}{9}|1 + 2e^{j\psi} + 3e^{j2\psi} + 2e^{j3\psi} + e^{j4\psi}|$$
$$= \tfrac{1}{9}|e^{j2\psi}[3 + 2(e^{j\psi} + e^{-j\psi}) + (e^{j2\psi} + e^{-j2\psi})]| \quad (11–96)$$
$$= \tfrac{1}{9}|3 + 4\cos\psi + 2\cos 2\psi|.$$

The graph of $|A(\psi)|$ versus ψ is shown in Fig. 11–15(a). Note that this figure holds for a general $\psi = \beta d \cos\phi + \xi$; the values of βd and ξ have not yet been specified.

In order to plot the desired radiation pattern we use the following additional information:

$$\text{Broadside radiation, } \zeta = 0: \quad \psi = \beta d \cos\phi;$$

$$\text{Element spacing, } d = \frac{\lambda}{2}: \quad \psi = \pi \cos\phi.$$

The normalized radiation pattern can be plotted from

$$|A(\phi)| = \tfrac{1}{9}|3 + 4\cos(\pi\cos\phi) + 2\cos(2\pi\cos\phi)|.$$

However, having calculated and plotted $|A(\psi)|$, we do not need to recalculate the array factor as a function of ϕ. This conversion can be effected graphically as follows (see Fig. 11–15):

1. Extend the vertical axis of the array-factor graph downward, and let it intersect with a horizontal line (which represents the line for $\phi = 0$ and $\phi = \pi$). The point of intersection is the point for $\xi = 0$.

2. Locate the point, P_0, on the horizontal line that is ξ radians to the right or left of the point of intersection, depending on whether ξ is positive or negative. (In the present case, $\xi = 0$ and P_0 is at the point of intersection.)

3. Using P_0 as the center, draw a circle with βd as the radius.

4. For any angle ϕ_1, draw the radius vector $P_0 P_1$. (The projection $P_0 P_1'$ is equal to $\psi_1 = \beta d \cos \phi_1$.)

5. At ψ_1, measure the magnitude of $|A(\psi_1)|$, which is marked as P_2 on the radius vector $P_0 P_1$. (P_2 is a point on the normalized radiation pattern.)

Repeat this process until the entire radiation pattern is obtained.

Figure 11–15(b) shows the normalized radiation pattern of this five-element broadside array with tapered excitation. The first sidelobe level is found to be 0.11
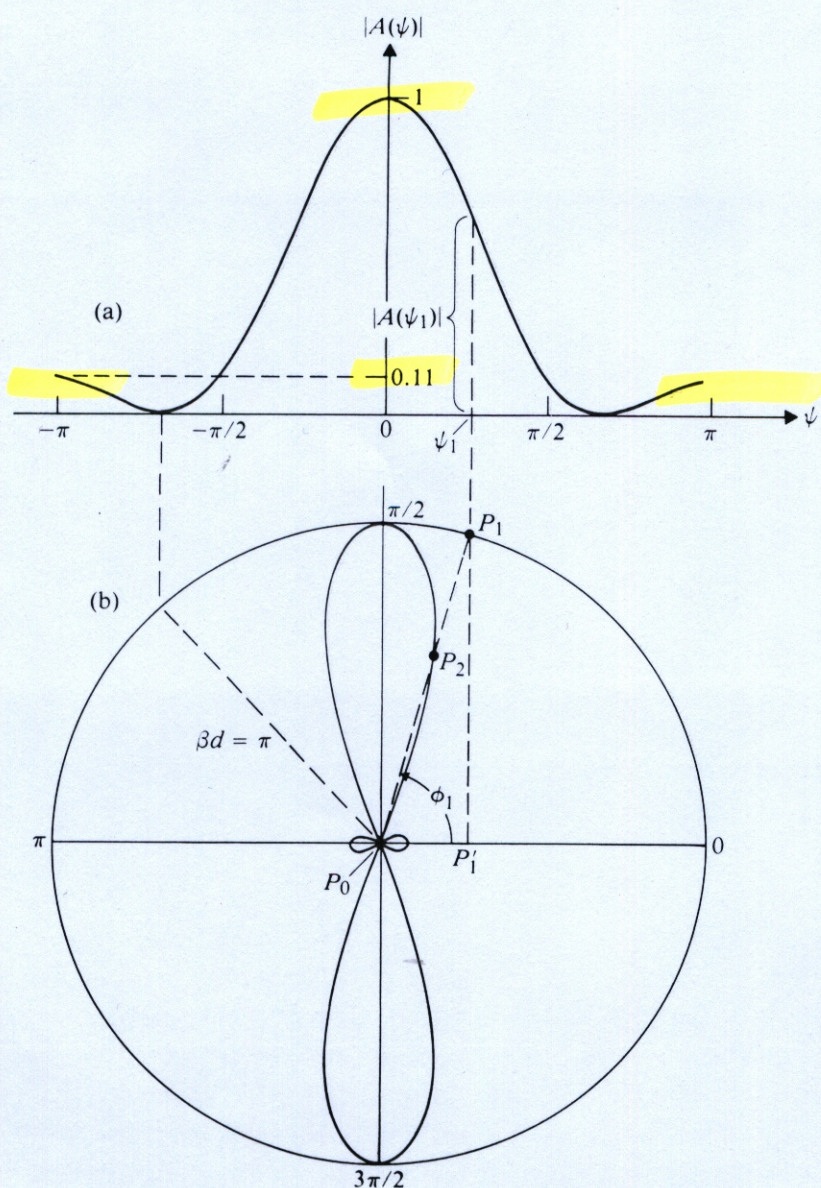

FIGURE 11–15
(a) Graph for normalized array factor as a function of ψ, and (b) normalized polar radiation pattern of a five-element broadside array with $d = \lambda/2$ and tapered excitation amplitude ratios 1:2:3:2:1 (Example 11–9).

or 20 $\log_{10}$ (1/0.11) = 19.2 (dB) down from the main-beam radiation. This compares with 0.25 or 12 (dB) down for the five-element uniform broadside array shown in Fig. 11–14.   ▬

In the discussion of uniform linear arrays we started out with the assumptions of equal spacing, equal excitation amplitude, and constant progressive phase shifts. The main reason for making these assumptions is mathematical simplicity in analyzing radiation characteristics. The preceding example shows that a tapered nonuniform amplitude distribution in the array elements produces the desirable result of a reduction in the sidelobe level. In a similar manner the spacings between neighboring elements may be made unequal [1]–[4], and the phase shifts do not have to be constant [5]. In two-dimensional arrays the elements need not be arranged in a rectangular lattice [6], [7]. We have, then, many additional parameters that can be adjusted to achieve desirable results. Adjustments in these parameters, however, destroy the simplicity of the analysis. There are techniques for synthesizing an antenna array to approximate a specified radiation pattern closely. It is not possible to examine all the various possible array designs in this book, but they do exist and present themselves as interesting problems [8]–[12].

Our discussions on linear arrays can be extended to two-dimensional rectangular arrays. A rectangular array can be studied as an array of linear arrays, to which the principle of pattern multiplication applies. From Eq. (11–90) we note that the direction of the main beam of a uniform linear array can be changed by simply changing the amount of progressive phase shift ξ. In fact, the radiation pattern can be changed from broadside ($\xi = 0$) to endfire ($\xi = -\beta d$) or to somewhere in between. We see here a possibility of *scanning* the main beam by simply varying ξ. This can be achieved in practice by using electronically controlled phase shifters. Antenna arrays equipped with phase shifters to steer the main beam electronically are called ***phased arrays***. The main beam of a two-dimensional array can be made to scan in both θ (elevation) and ϕ (azimuth) directions. Scanning phased arrays are of great practical importance in radar and radioastronomy work, in which the antenna system may be arrays of many thousands of elements that are not amenable to rapid mechanical motion for beam steering. Time-delay circuits may also be used to furnish the required phase shifts to the various array elements. By changing the frequency the time-delays are translated into varying phase shifts. This scheme is called ***frequency scanning***.

11–6 Receiving Antennas

In the discussion of antennas and antenna arrays so far we have implied that they operate in a transmitting mode. In the transmitting mode a voltage source is applied to the input terminals of an antenna, setting up currents and charges on the antenna structure. The time-varying currents and charges, in turn, radiate electromagnetic waves, which carry energy and/or information. A transmitting antenna can then be regarded as a device that transforms energy from a source (a generator) to energy
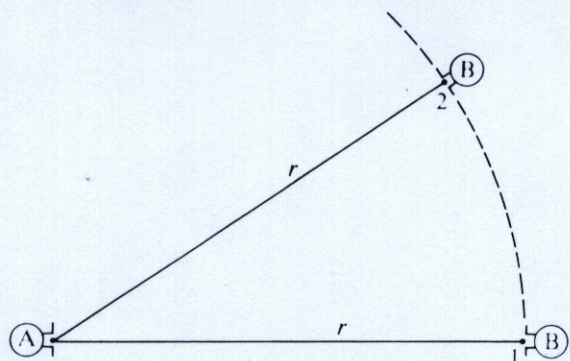
FIGURE 11–16
Two coupled antennas.

associated with an electromagnetic wave. A receiving antenna, on the other hand, extracts energy from an incident electromagnetic wave and delivers it to a load. In the receiving mode the external electromagnetic field that causes currents and charges to flow is incident on the entire antenna structure, not just at the input terminals. Moreover, the induced currents and charges, which depend on the direction of arrival of the incident electromagnetic wave, will produce reradiation or scattering of electromagnetic energy, making the situation very complicated. We may reasonably expect that the current and charge distributions on an antenna in the receiving mode are different from those in the transmitting mode. Nevertheless, despite these differences, reciprocity relations enable us to conclude that (1) the equivalent generator impedance of an antenna in the receiving mode is equal to the input impedance of the antenna in the transmitting mode, and (2) the directional pattern of an antenna for reception is identical with that for transmission. We will justify these two important conclusions by using equivalent network representations. Also in this section we will discuss the concepts of effective area and backscatter cross section.

11–6.1 INTERNAL IMPEDANCE AND DIRECTIONAL PATTERN

Let us assume that a transmitter with antenna A radiates electromagnetic energy, which is absorbed by a distant receiver with antenna B. Antenna B moves about antenna A at a constant distance r[†] and is always oriented in such a way as to receive maximum power, as illustrated in Fig. 11–16. The two coupled antennas and the space between can be represented as a two-port T-network shown in Fig. 11–17. The terminal characteristics, (V_1, I_1) and (V_2, I_2) of antennas A and B, respectively, are linearly related by the following equations:

$$V_1 = Z_{11}I_1 + Z_{12}I_2, \tag{11–97}$$
$$V_2 = Z_{21}I_1 + Z_{22}I_2, \tag{11–98}$$

where Z_{11}, Z_{12}, Z_{21}, and Z_{22} are open-circuit impedance coefficients.

---

† The symbol r, instead of R, is used here to denote distance in order to avoid possible confusion of the latter with the symbol for resistance used later in this chapter.
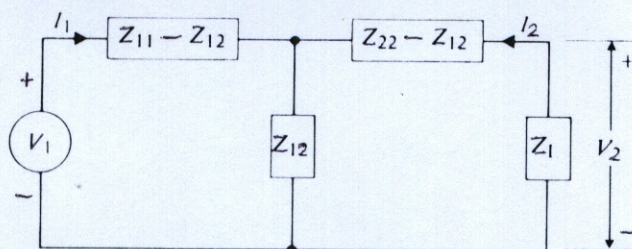
When the medium in the transmission path between antennas A and B is bilateral such that reciprocity relations hold, the transfer or coupling impedances Z_{12} and Z_{21} are equal.[†] Under normal circumstances, transmitting and receiving antennas are separated by very large distances, and the coupling impedances are negligibly small as far as *the reaction on the transmitting antenna* owing to scattering by the receiving antenna is concerned. In the limit $r \to \infty$,

$$\lim_{r \to \infty} Z_{12} = 0. \tag{11-99}$$

The parallel arm of the T-network in Fig. 11-17 is almost a short-circuit, and the impedance coefficients Z_{11} and Z_{22} are nearly equal to the input impedances Z_A and Z_B, respectively, of isolated antennas A and B in the transmitting mode. Equation (11-97) can be written approximately as

$$V_1 \cong Z_{11}I_1 \cong Z_A I_1. \tag{11-100}$$

An equivalent circuit representing Eq. (11-100) is drawn in Fig. 11-18(a).

The coupling *from* the transmitting antenna *to* the receiving antenna, however, cannot be neglected inasmuch as it is through this coupling that the latter extracts energy from the electromagnetic wave originated from the former. Thévenin's theorem can be applied to the left of the load impedance Z_L in the network in Fig. 11-17 to determine an open-circuit voltage V_{oc} and an internal impedance Z_g. An equivalent circuit at the receiving end is shown in Fig. 11-18(b). We have

$$V_{oc} = \frac{Z_{12}}{Z_{11}} V_1, \tag{11-101}$$

$$Z_g = (Z_{22} - Z_{12}) + \frac{Z_{12}}{Z_{11}}(Z_{11} - Z_{12}) = Z_{22} - \frac{Z_{12}^2}{Z_{11}}. \tag{11-102}$$

(Z₁₂/ Z₁₁)

Because of the weak coupling, we conclude that *the equivalent generator internal impedance Z_g for antenna B in the receiving mode is* approximately equal to its input impedance when it is transmitting; that is,

$$Z_g \cong Z_{22} \cong Z_B. \tag{11-103}$$

[†] An example of a nonbilateral medium for which $Z_{12} \neq Z_{21}$ is the ionosphere under the influence of the earth's magnetic field.
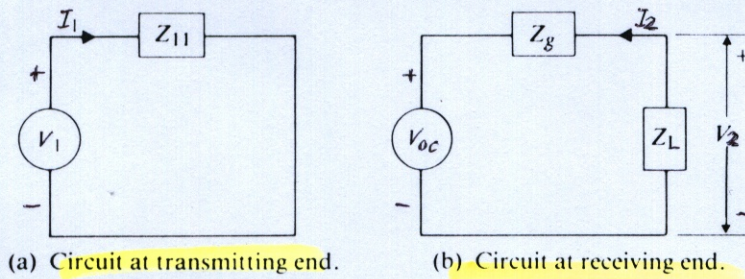
(a) Circuit at transmitting end.   (b) Circuit at receiving end.

FIGURE 11–18
Approximate equivalent circuits for weakly coupled antennas.

When antenna B is receiving, $V_2 = -I_2 Z_L$, and Eq. (11–98) becomes

$$I_2 = -\frac{Z_{21}}{Z_{22} + Z_L} I_1. \tag{11–104}$$

The time-average power absorbed in Z_L is

$$P_L = \frac{1}{2} \mathscr{R}e[-V_2 I_2^*] = \frac{|I_1|^2}{2} \left| \frac{Z_{21}}{Z_{22} + Z_L} \right|^2 \mathscr{R}e(Z_L). \tag{11–105}$$

For two successive positions of antenna B as indicated in Fig. 11–16 the ratio of the absorbed powers in Z_L is

$$\frac{P_L(\theta_1, \phi_1)}{P_L(\theta_2, \phi_2)} = \left| \frac{Z_{21}(\theta_1, \phi_1)}{Z_{21}(\theta_2, \phi_2)} \right|^2. \tag{11–106}$$

Thus the absorbed power is proportional to the square of the transfer impedance coefficient.

If we consider the situation in which antenna B is transmitting and antenna A is receiving, then the ratio of the absorbed powers in Z_L connected to antenna A for the two successive locations of antenna B would be the same as that given in Eq. (11–106), except that Z_{21} would be replaced by Z_{12}. Because of the reciprocity relation $Z_{12} = Z_{21}$, we conclude that *the directional pattern of an antenna for reception is identical with that for transmission*.

11–6.2   EFFECTIVE AREA

In discussing receiving antennas it is convenient to define a quantity called the *effective area*.[†] The effective area, A_e, of a receiving antenna is the ratio of the average power delivered to a *matched load* to the time-average power density (time-average Poynting vector) of the incident electromagnetic wave at the antenna. We write

$$P_L = A_e \mathscr{P}_{av}, \tag{11–107}$$

where P_L is the maximum average power transferred to the load (under matched conditions) with the receiving antenna properly oriented with respect to the polariza-

---

[†] Also called *effective aperture* or *receiving cross section*.

tion of the incident wave. We will now show that the effective area bears a definite relationship with the directive gain of an antenna.

When the load impedance is matched to the internal impedance,

$$Z_L = Z_g^* \cong R_B - jX_B, \tag{11-108}$$

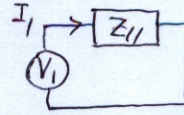the maximum power delivered to the load is, from Eq. (11-105), (and (11-103))

$$P_L = \frac{|I_1|^2}{2} \left| \frac{Z_{21}}{Z_{22} + Z_L} \right|^2 Re(Z_L) \xrightarrow{Z_g \cong Z_{22}} \qquad P_L = \frac{|I_1 Z_{21}|^2}{8R_B}. \tag{11-109}$$

Let R_A be the input resistance of transmitting antenna A. The transmitted power is then

$$P_t = \tfrac{1}{2}|I_1|^2 R_A. \qquad (Fig. \ 11-18(a)) \tag{11-110}$$

Combining Eqs. (11-109) and (11-110), we have

$$\frac{P_L}{P_t} = \frac{|Z_{21}|^2}{4R_A R_B}. \tag{11-111}$$

When antenna B is receiving, the time-average power density at B depends on the directive gain of transmitting antenna A in that direction:

$$U = R^2 \mathscr{P}_{av} \quad (11-32)$$
$$G_D = 4\pi U/P_r \quad (11-34)$$
$$\Bigg\} \Rightarrow \qquad \mathscr{P}_{av} = \frac{P_t}{4\pi r^2} G_{DA}. \tag{11-112}$$

Using Eq. (11-112) in Eq. (11-107), we obtain

$$\frac{P_L}{P_t} = \frac{A_{eB} G_{DA}}{4\pi r^2}. \tag{11-113}$$

Comparison of Eqs. (11-111) and (11-113) yields

$$|Z_{21}|^2 = \frac{R_A R_B A_{eB} G_{DA}}{\pi r^2}. \tag{11-114}$$

If antenna B is transmitting and antenna A is receiving, a similar derivation leads to

$$|Z_{12}|^2 = \frac{R_B R_A A_{eA} G_{DB}}{\pi r^2}. \tag{11-115}$$

Since $Z_{12} = Z_{21}$, Eqs. (11-114) and (11-115) lead to the following important relation:

$$\frac{G_{DA}}{A_{eA}} = \frac{G_{DB}}{A_{eB}}. \tag{11-116}$$

Inasmuch as we have not specified the types of transmitting and receiving antennas in obtaining Eq. (11-116), we conclude that *the ratio of the directive gain and the effective area of an antenna is a universal constant*. This constant can be found by determining the directive gain and effective area of any antenna—for instance, those of an elemental dipole as illustrated in the following example.

(Fig. 11-8)'

$V_{oc} = E_i \, d\ell \sin\theta$

$P_r = \frac{1}{2} I^2 R_r$
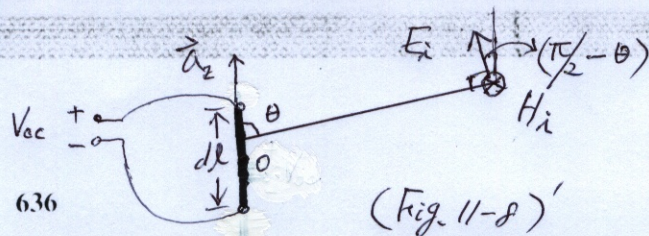
EXAMPLE 11–10   Determine the effective area, $A_e(\theta)$, of an elemental electric dipole of a length $d\ell$ ($\ll \lambda$) used to receive an incident plane electromagnetic wave of wavelength λ that is polarized in a direction shown in Fig. 11–8.

Solution   Let E_i be the amplitude of the electric field intensity at an elemental dipole of length $d\ell$. Then the time-average power density is

$$\mathscr{P}_{av} = \frac{E_i^2}{2\eta_0}. \tag{11–117}$$

The average power delivered to a matched load ($Z_L = Z_g^*$) is

$$P_L = \frac{1}{2}\left|\frac{E_i \, d\ell \sin\theta}{Z_g + Z_g^*}\right|^2 R_r = \frac{(E_i \, d\ell)^2 \sin^2\theta}{8R_r}, \tag{11–118}$$

where $R_r = 80(\pi \, d\ell/\lambda)^2$ has been given in Eq. (11–44). The ratio $P_L/\mathscr{P}_{av}$ gives the effective area of the elemental dipole:

$$A_e(\theta) = \frac{P_L}{\mathscr{P}_{av}} = \frac{\eta_0}{4R_r}(d\ell)^2 \sin^2\theta$$

$$= \frac{3}{8\pi}(\lambda \sin\theta)^2 \quad (\text{m}^2). \tag{11–119}$$

It is interesting to note that the effective area of an elemental electric dipole is independent of its length.

From Example 11–2 we have $G_D(\theta) = \frac{3}{2}\sin^2\theta$ for an elemental electric dipole. Thus,

$$G_D(\theta) = \frac{3}{2}\sin^2\theta = \frac{4\pi}{\lambda^2}\frac{3}{8\pi}(\lambda \sin\theta)^2 \tag{11–120}$$

$$= \frac{4\pi}{\lambda^2}A_e(\theta),$$

which indicates that the universal constant for Eq. (11–116) is $4\pi/\lambda^2$, and we may write the following relation for an antenna under matched impedance conditions:

$$\boxed{G_D(\theta, \phi) = \frac{4\pi}{\lambda^2}A_e(\theta, \phi) \qquad \text{(Dimensionless)}.} \tag{11–121}$$

In the case of thin linear antennas the concept of effective area may seem arbitrary. Nevertheless, its definition is useful in measuring the power available to a particular antenna. Of course, we expect the effective area $A_e(\theta)$ to be related to the effective length $\ell_e(\theta)$. The available power to the antenna load under matched conditions is

$$P_L = \frac{V_{oc}^2}{8R_r} = \frac{(-\ell_e E_i)^2}{8R_r}, \tag{11–122}$$

where the relation in Eq. (11–75) has been used. Substitution of Eqs. (11–117) and (11–122) into Eq. (11–107) yields

$$A_c(\theta) = \frac{30\pi}{R_r} \ell_c^2(\theta). \tag{11–123}$$

11–6.3   BACKSCATTER CROSS SECTION

As we saw in the preceding subsection, the concept of effective area pertains to the power available to the matched load of a receiving antenna for a given incident power density. In cases in which the incident wave impinges on a passive object whose purpose is not to extract energy from the incident wave but whose presence creates a scattered field, it is appropriate to define a quantity called the **backscatter cross section**, or **radar cross section**. The backscatter cross section of an object is the equivalent area that would intercept that amount of incident power in order to produce the same scattered power density at the receiver site if the object scattered uniformly (isotropically) in all directions. Let

$\mathcal{P}_i$ = Time-average incident power density at the object   (W/m^2),

$\mathcal{P}_s$ = Time-average scattered power density at the receiver site   (W/m^2),

σ_{bs} = Backscatter cross section   (m^2),

r = Distance between scatterer and receiver   (m).

Then,

$$\frac{\sigma_{bs}\mathcal{P}_i}{4\pi r^2} = \mathcal{P}_s$$

or

$$\sigma_{bs} = 4\pi r^2 \frac{\mathcal{P}_s}{\mathcal{P}_i} \quad (\text{m}). \tag{11–124}$$

Note that $\mathcal{P}_s$ is inversely proportional to r^2 for large r and that σ_{bs} does not change with r.

The backscatter cross section is a measure of the detectability of the object (target) by **radar** (**ra**dio **d**etection **a**nd **r**anging); hence the term radar cross section. It is a composite measure, depending on the geometry, orientation, and constitutive parameters of the object, and on the frequency and polarization of the incident wave in a complicated way.

EXAMPLE 11–11   A uniform plane wave with electric field intensity $\mathbf{E}_i = \mathbf{a}_z E_i$ impinges on a small dielectric sphere of radius $b \, (\ll \lambda)$ and dielectric constant ϵ_r, as shown in Fig. 11–19. Assume the polarization produced in the sphere to be the same
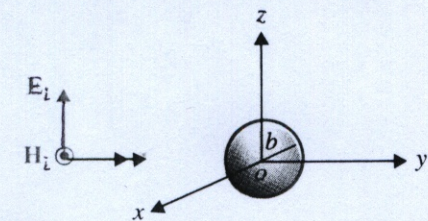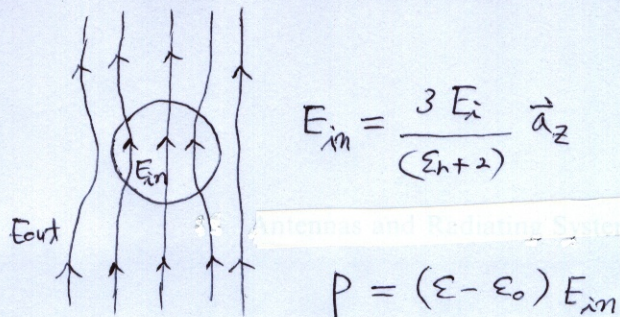
$$\vec{E}_i(\vec{r}, t) = Re[E_i \, e^{j\omega t}]$$

$$E_{in} = \frac{3 E_i}{(\epsilon_h + 2)} \vec{a}_z$$

$$P = (\epsilon - \epsilon_0) E_{in}$$

638

$$\vec{E}_i(\vec{r}, t) = \mathcal{R}e[E_i e^{j\omega t}], \quad E_i = \vec{a}_z E_i, \quad b \ll \lambda$$

FIGURE 11–19
Plane wave incident on a small dielectric sphere.

as that produced in a uniform static electric field $\mathbf{E}_i$ and to be given by (see Problem P.4–29)

$$\mathbf{P} = \epsilon_0(\epsilon_r - 1)\mathbf{E}$$
$$= \mathbf{a}_z 3\epsilon_0 \left(\frac{\epsilon_r - 1}{\epsilon_r + 2}\right) E_i \quad (\text{C/m}^2). \tag{11–125}$$
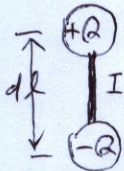
a) Find the backscatter cross section σ_{bs}.
b) Determine σ_{bs} for a spherical raindrop of diameter 3 (mm) at 15 (GHz), assuming the dielectric constant of water to be 55 at that frequency.

Solution

a) Since the induced polarization vector (the volume density of electric dipole moment) $\mathbf{P}$ is constant within the dielectric sphere, the total electric dipole moment induced in the sphere of radius $b (\ll \lambda)$ is

$$\mathbf{p} = \tfrac{4}{3}\pi b^3 \mathbf{P}$$

$P = Q \, d\ell = \frac{I}{j\omega} d\ell$ (11-10) (11-11)

$$= \mathbf{a}_z 4\pi b^3 \epsilon_0 \left(\frac{\epsilon_r - 1}{\epsilon_r + 2}\right) E_i \quad (\text{C·m}). \tag{11–126}$$

Thus the dielectric sphere acts electromagnetically like an elemental electric dipole of moment $\mathbf{p}$ given in Eq. (11–126). The scattered electric field intensity in the far-zone is then, from Eq. (11–19b) and using Eqs. (11–10) and (11–11),

$E_\theta = j \frac{I d\ell}{4\pi}\left(\frac{e^{-j\beta R}}{R}\right)$
$\times \eta_0 \beta \sin\theta$ (11-19b)

$$\mathbf{E}_s = \mathbf{a}_\theta E_s = -\mathbf{a}_\theta \frac{\omega p}{4\pi}\left(\frac{e^{-j\beta r}}{r}\right)\eta_0 \beta \sin\theta$$
$$= -\mathbf{a}_\theta \beta^2 b^3 \left(\frac{e^{-j\beta r}}{r}\right)\left(\frac{\epsilon_r - 1}{\epsilon_r + 2}\right) E_i \sin\theta \quad (\text{V/m}). \tag{11–127}$$

The time-average backscattered power density is

$$\mathscr{P}_s = \frac{1}{2\eta_0}|E_s|^2_{\theta=\pi/2} = \frac{b^2(\beta b)^4}{2\eta_0 r^2}\left(\frac{\epsilon_r - 1}{\epsilon_r + 2}\right)^2 E_i^2 \quad (\text{W/m}^2). \tag{11–128}$$

The time-average incident power density is

$$\mathscr{P}_i = \frac{1}{2\eta_0} E_i^2 \quad (\text{W/m}^2). \tag{11–129}$$

Substitution of Eqs. (11–128) and (11–129) in Eq. (11–124) yields the backscatter cross section:

$$\sigma_{bs} = 4\pi b^2 (\beta b)^4 \left(\frac{\epsilon_r - 1}{\epsilon_r + 2}\right)^2 \qquad (m^2). \qquad (11-130)$$

b) For $f = 15$ (GHz), $\lambda = 20$ (mm), the radius of the raindrop $b = \frac{3}{2}$ (mm) $\ll \lambda$. We obtain

$$\sigma_{bs} = 1.25 \times 10^{-6} \quad (m^2)$$
$$= 1.25 \quad (mm^2),$$

which is a fraction of the geometrical cross section πb^2 of the sphere:

$$\frac{\sigma_{bs}}{\pi b^2} = \frac{1.25}{1.5^2 \pi} = 0.177.$$

Of course, raindrops do not exist singly; nor is their shape strictly spherical. Meaningful calculations of backscatter from rain require a knowledge of the rainfall rate and the distribution of the drop size, which are mutually dependent. The assumption of an equivalent spherical drop for nonspherical droplets has been found to be acceptable as long as their sizes are much smaller than the wavelength. Of equal importance to the calculation of backscatter from rainfall is the estimation of the attenuation suffered by an electromagnetic wave propagating through rain due to an imaginary part of the permittivity of raindrops. Interested readers should refer to the literature for details. [13]

11–7 Transmit-Receive Systems

In the preceding section we discussed the concepts of effective area for receiving antennas and backscatter cross section for scattering objects. We shall now examine the power transmission relation between transmitting and receiving antennas. When the same antenna is used for transmitting short pulses of radiation and for receiving them after they have been reflected (scattered) back by a target, the transmit-receive system is a *radar*; it is a special case. Measurement of the time elapsed Δt between the transmitted pulse and the received pulse determines the distance r of the target to the antenna site through the relation $\Delta t = 2r/c$, where c is the velocity of light.

If the transmission path between the transmitting and receiving antennas is near the earth's surface, the effect of the conducting earth must be considered. We shall also discuss the transmit-receive arrangement over a flat earth in this section.

11–7.1 FRIIS TRANSMISSION FORMULA AND RADAR EQUATION

Consider a communication circuit between stations 1 and 2 with antennas having effective areas A_{e1} and A_{e2}, respectively. The antennas are separated by a distance r. We wish to find a relation between the transmitted and the received powers.

Let P_L and P_t be the received and transmitted powers, respectively. Combining Eqs. (11–113) and (11–121), we obtain

$$\frac{P_L}{P_t} = \left(\frac{A_{e2}}{4\pi r^2}\right)G_{D1} = \left(\frac{A_{e2}}{4\pi r^2}\right)\left(\frac{4\pi A_{e1}}{\lambda^2}\right)$$

or

$$\boxed{\frac{P_L}{P_t} = \frac{A_{e1}A_{e2}}{r^2\lambda^2}.} \qquad (11\text{–}131)$$

The relation in Eq. (11–131) is referred to as the **Friis transmission formula**. For a given transmitted power the received power is directly proportional to the product of the effective areas of the transmitting and receiving antennas and is inversely proportional to the square of the product of the distance of separation and wavelength.

Noting Eq. (11–121), we may write the Friis transmission formula in the following alternative form:

$$\boxed{\frac{P_L}{P_t} = \frac{G_{D1}G_{D2}\lambda^2}{(4\pi r)^2}.} \qquad (11\text{–}132)$$

The received power P_L in Eqs. (11–131) and (11–132) assumes a matched condition and disregards the power dissipated in the antenna itself. From Eq. (11–131) we see that for a given transmitted power the received power increases as the square of the operating frequency (decreases as the inverse square of wavelength). But, at progressively increasing frequencies, P_t is limited by available technology, and the minimum detectable power over electromagnetic noise also increases. It is incorrect to conclude from Eq. (11–132) that P_L increases as the square of the wavelength because the directive gains usually decrease as the wavelength increases.

Now consider a radar system that uses the same antenna for transmitting short pulses of time-harmonic radiation and for receiving the energy scattered back from a target. For a transmitted power P_t the power density at a target at a distance r away is (see Eq. 11–112)

$$\mathscr{P}_T = \frac{P_t}{4\pi r^2}\,G_D(\theta, \phi), \qquad (11\text{–}133)$$

where $G_D(\theta, \phi)$ is the directive gain of the antenna in the direction of the target. If σ_{bs} denotes the backscatter or radar cross section of the target, then the equivalent power that is scattered isotropically is $\sigma_{bs}\mathscr{P}_T$, which results in a power density at the antenna $\sigma_{bs}\mathscr{P}_T/4\pi r^2$. Let A_e be the effective area of the antenna. We have the following expression for the received power:

$$
\begin{aligned}
P_L &= A_e\sigma_{bs}\frac{\mathscr{P}_T}{4\pi r^2} \\[2mm]
&= A_e\sigma_{bs}\frac{P_t}{(4\pi r^2)^2}\,G_D(\theta, \phi).
\end{aligned}
\qquad (11\text{–}134)
$$

By using Eq. (11-121), Eq. (11-134) becomes

$$\boxed{\frac{P_L}{P_t} = \frac{\sigma_{bs}\lambda^2}{(4\pi)^3 r^4} G_D^2(\theta, \phi),}$$

(11-135)

which is called the *radar equation*. In terms of the antenna effective area A_e instead of the directive gain $G_D(\theta, \phi)$, the radar equation can be written as

$$\boxed{\frac{P_L}{P_t} = \frac{\sigma_{bs}}{4\pi}\left(\frac{A_e}{\lambda r^2}\right)^2.}$$

(11-136)

Because radar signals have to make round trips from the antenna to the target and then back to the antenna, the received power is inversely proportional to the fourth power of the distance r of the target from the antenna.

EXAMPLE 11-12 Assume that 50 (kW) is fed into the antenna of a radar system operating at 3 (GHz). The antenna has an effective area of 4 (m²) and a radiation efficiency of 90%. The minimum detectable signal power (over noise inherent in the receiving system and from the environment) is 1.5 (pW), and the power reflection coefficient for the antenna on receiving is 0.05. Determine the maximum usable range of the radar for detecting a target with a backscatter cross section of 1 (m²).

Solution At $f = 3 \times 10^9$ (Hz), $\lambda = 0.1$ (m):

$$A_e = 4 \quad (m^2),$$
$$P_t = 0.90 \times 5 \times 10^4 = 4.5 \times 10^4 \quad (W),$$
$$P_L = 1.5 \times 10^{-12}\left(\frac{1}{1 - 0.05}\right) = 1.58 \times 10^{-12} \quad (W),$$
$$\sigma_{bs} = 1 \quad (m^2).$$

From Eq. (11-136),

$$r^4 = \frac{\sigma_{bs}A_e^2}{4\pi\lambda^2}\left(\frac{P_t}{P_L}\right),$$

and

$$r = 4.36 \times 10^4 \text{ (m)} = 43.6 \quad (km).$$

A satellite communication system makes use of satellites traveling in orbits in the earth's equatorial plane. The speed of the satellites and the radius of their orbits are such that the period of rotation of the satellites around the earth is the same as that of the earth. Thus the satellites appear to be stationary with respect to the earth's surface, and they are said to be geostationary. The radius of the geosynchronous orbit is 42,300 (km). With an earth radius of 6380 (km) the satellites are about 36,000 (km) from the earth's surface.

Signals are transmitted from a high-gain antenna at an earth station toward a satellite, which receives the signals, amplifies them, and retransmits them back toward the earth station at a different frequency. Three satellites equally spaced around the geosynchronous orbit would cover almost the entire earth's surface except the polar regions (see Problem P.11–27). A quantitative analysis of the power and antenna gain relations for a satellite communication circuit requires the application of the Friis transmission formula twice, once for the uplink (earth station to satellite) and once for the downlink (satellite to earth station).

11–7.2   WAVE PROPAGATION NEAR EARTH'S SURFACE

Consider a transmitting antenna A at a height h_1 and a receiving antenna B at a height h_2 above the flat earth's surface with a distance of separation d, as shown in Fig. 11–20. If antenna A is an elemental electric dipole, then the electric field intensity at B is the sum of the direct contribution $\mathbf{E}_{\theta 1}$ from A and the indirect contribution $\mathbf{E}_{\theta 2}$ after reflection at point C. We write

$$\mathbf{E} = \mathbf{E}_{\theta 1} + \mathbf{E}_{\theta 2}, \tag{11–137}$$

where the magnitudes of $\mathbf{E}_{\theta 1}$ and $\mathbf{E}_{\theta 2}$ are

$$E_{\theta 1} = K\left(\frac{e^{-j\beta R}}{R}\right)\sin\theta, \tag{11–137a}$$

$$E_{\theta 2} = K\left(\frac{e^{-j\beta R'}}{R'}\right)\sin\theta'. \tag{11–137b}$$

The constant K equals $jI\,d\ell\eta_0\beta/4\pi$ (see Eq. 11–19b), and the distance $R' = \overline{AC} + \overline{CB} = \overline{A'B}$. The effect of the perfectly conducting (assumed) earth's surface is replaced by an image antenna at A'. In the general case, $\mathbf{E}_{\theta 1}$ and $\mathbf{E}_{\theta 2}$ are not parallel; but if $d \gg h_1, h_2$, then $\theta \cong \theta'$, and Eqs. (11–137a) and (11–137b) may be combined to give

$$E_\theta \cong \mathbf{a}_\theta K\left(\frac{e^{-j\beta R}}{R}\right)(\sin\theta)F, \tag{11–138}$$
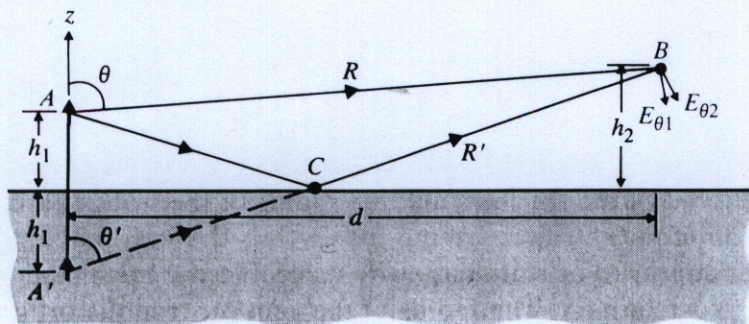

FIGURE 11–20
Transmit-receive system near the earth's surface.

where

$$F = 1 + e^{-j\beta(R'-R)}. \qquad (11\text{-}139)$$

The distances

$$
\begin{aligned}
R &= [d^2 + (h_2 - h_1)^2]^{1/2} \\
&= d\left[1 + \frac{(h_2 - h_1)^2}{d^2}\right]^{1/2} \cong d + \frac{(h_2 - h_1)^2}{2d} \qquad (11\text{-}140a)
\end{aligned}
$$

and

$$R' = [d^2 + (h_2 + h_1)^2]^{1/2} \cong d + \frac{(h_2 + h_1)^2}{2d} \qquad (11\text{-}140b)$$

yield approximately

$$
\begin{aligned}
R' - R &\cong \frac{(h_2 + h_1)^2}{2d} - \frac{(h_2 - h_1)^2}{2d} \\
&= \frac{2h_1 h_2}{d}.
\end{aligned} \qquad (11\text{-}141)
$$

Substituting Eq. (11-141) in Eq. (11-139), we obtain

$$|F| = |1 + e^{-j\beta 2h_1 h_2/d}|, \qquad (11\text{-}142)$$

which is like the array factor of a two-element array.

Equation (11-142) may be written as

$$|F| = |e^{-j\beta h_1 h_2/d}(e^{j\beta h_1 h_2/d} + e^{-j\beta h_1 h_2/d})| = 2\left|\cos\left(\frac{2\pi h_1 h_2}{\lambda d}\right)\right|. \qquad (11\text{-}143)$$

Equation (11-143) shows that for fixed values of h_1 and λ the electric field intensity E_θ at the receiving site B will have nulls and maximum values as the ratio h_2/d is changed. The quantity $|F|$ varies from 0 to 2 and is called the **path-gain factor**. Calculation of the path-gain factor for a spherical earth is a much more involved task.

11-8 Some Other Antenna Types

Practical antennas take many different shapes and sizes, each designed to fulfill certain desired performance characteristics. Our attention so far has been focused on the radiation properties of linear antennas having a current distribution in the form of a standing wave. In this section we shall discuss several other types of antennas of practical importance.

11-8.1 TRAVELING-WAVE ANTENNAS

In the analysis of thin linear antennas in Section 11-4 we assumed that the center-driven dipole antennas were not terminated and that the currents from the excitation